LiDAR Remote Sensing Data Collection:
Lewis County, Washington

LiDAR-Derived Data: Point Cloud of Laser Returns Colored by Elevation and Intensity

Submitted to:

Jerry Harless
GIS Manager
Puget Sound Regional Council
1011 Western Avenue, Suite 500
Seattle, WA 98104-1035

Stearns Wood
GIS Manager
Lewis County Public Works Dept
350 N. Market Blvd.
Chehalis, WA 98532-2626

Phyllis A. Mann
Director
Kitsap County
911 Carver Street
Bremerton, WA 98312

Submitted by:

Watershed Sciences, Inc.
4605 NE Fremont, Suite 211
Portland, Oregon 97213

Watershed Sciences
Applied Remote Sensing & Analysis

September 19, 2006

LiDAR Remote Sensing Data Collection:
Lewis County, Washington

Table of Contents

Watershed Sciences
Applied Remote Sensing & Analysis

September 19, 2006

1. Introduction

Watershed Sciences, Inc. (WS) collected Light Detection and Ranging (LiDAR) data on March 19-20 and 27-29, 2006 of Lewis County, Washington. The survey area covers 254,439 acres primarily within Lewis County, with some overlap into neighboring counties (**Figure 1**).

Laser points were collected over the study area using an Optech ALTM 3100 LiDAR laser system set to acquire points at an average density of 4.5 points per square meter. Full overlap (i.e., ≥50% side-lap) ensured complete coverage and minimized laser shadows created by buildings and tree canopies. A real-time kinematic (RTK) ground survey was conducted throughout the study area for quality assurance purposes. The accuracy of the LiDAR data is described as standard deviations of divergence (sigma ~ σ) from RTK ground survey points and root mean square error (RMSE) which considers bias (upward or downward). The data have a 1σ of 0.20 feet, 2σ of 0.42 feet and an RMSE of 0.21 feet. Deliverables include point data, 2-foot resolution contours, 3-foot resolution laser intensity images, 3- and 6-foot resolution bare ground model ESRI GRIDs, and 3-foot resolution Fusion and Highest Hit vegetation model ESRI GRIDs for the entire study area. All data are delivered in Washington State Plane South Coordinate System FIPS 4602, in the NAD83(CORS96)/NAVD88 datum.

Figure 1. Full extent of Area of Interest (~254,439 Acres)

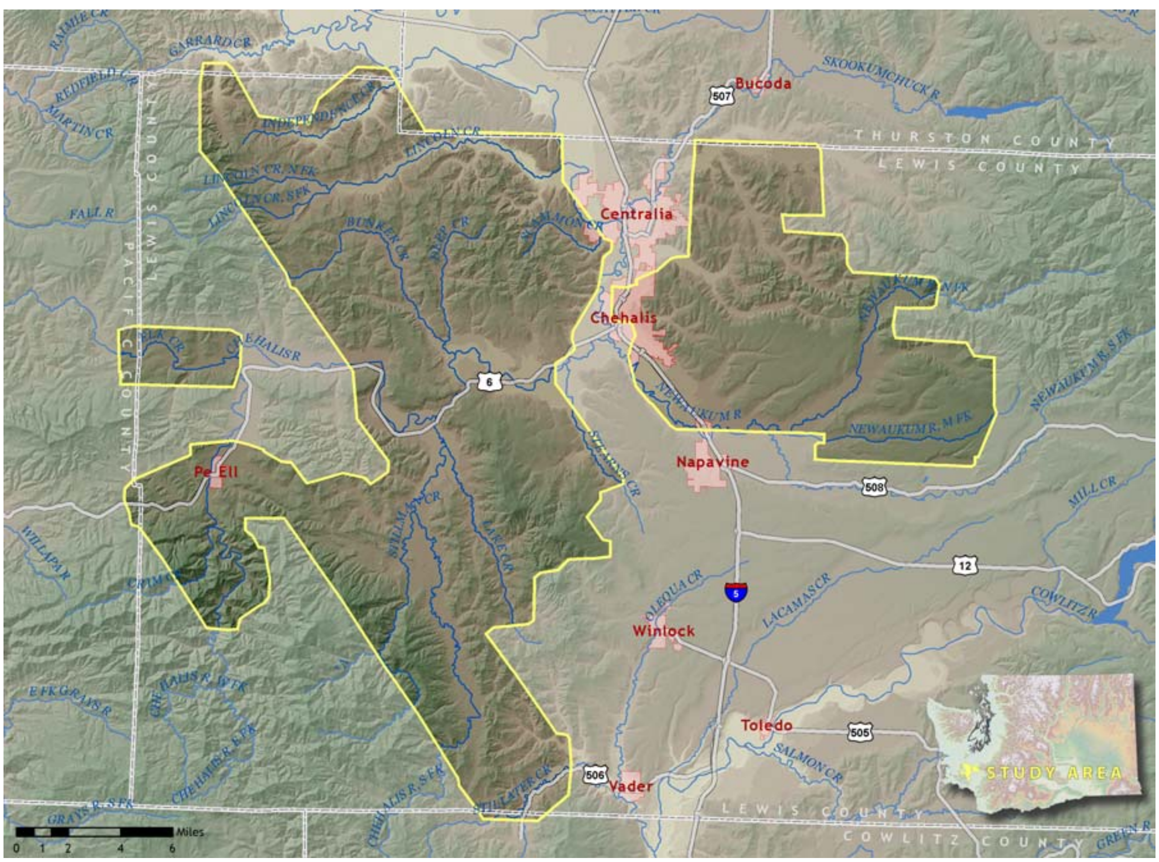

The delivered LiDAR data cover approximately 254,439 acres, while the original area of interest was delineated as 180,837 acres. Fixed-wing LiDAR acquisitions require straight and parallel flightlines planned with a minimal number of lines (to limit the aircraft turns at the end of the line). The delivered area is the result of the most efficient flight plan designed with these considerations that captures the area of interest. Therefore, to maximize Lewis County LiDAR flight efficiency, data were collected over continuous areas that exceeded the original study area. **Figure 2** below compares the delivered and original study areas.

Figure 2. The Original Area of Interest (~180,837 Acres) and the Delivered Study Area (~254,439 Acres)

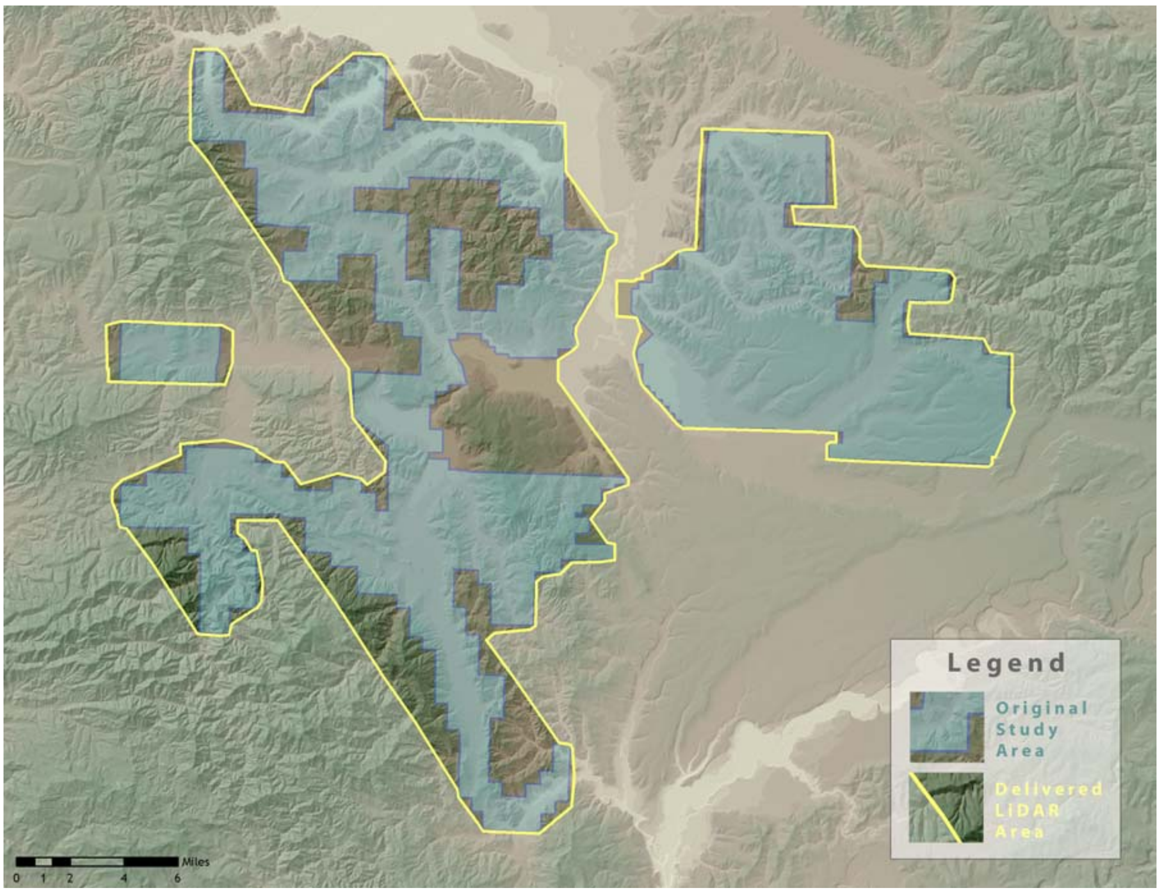

2. Acquisition

2.1 Airborne Survey – Instrumentation and Methods

The LiDAR survey utilized an Optech ALTM 3100 mounted in a Cessna Grand Caravan 208B. The survey was conducted on March 19-20 and 27-29, 2006. The LiDAR data acquisition specifications are listed below in **Table 1**.

Table 1. LiDAR Data Acquisition Specifications

Laser Pulse Repetition Rate:	71,000 pulses per second (71 kHz)
Operating Altitude:	1,200 m AGL
Flight Speed:	120 knots
Scan Angle:	±16° from Nadir
Scan Pattern:	Sawtooth
Laser Footprint Diameter on Ground:	33 cm
Number of Returns Collected Per Laser Pulse:	Up to 4
Native Pulse Density:	4.5 pulse/m^2
Intensity Range:	8 bits
Adjacent Swath Overlap (Side-Lap) :	≥50%
Vertical RMSE of LiDAR Survey:	0.21 feet
Number of GPS Base Stations Used:	2 per flight
Maximum Distance From Airborne to Ground GPS:	32 km (19.9 miles)
GPS PDOP During Acquisition:	≤3.0
GPS Satellite Constellation During Acquisition:	≥6
RTK Quality Control Data Points Collected:	1,522
RTK Data RMSE:	≤1.5 cm

The Optech ALTM 3100 LiDAR system was set to acquire 71,000 laser pulses per second (i.e. 71kHz pulse repetition rate) and flown at 1,200 meters above ground level (AGL), capturing a scan angle of ±16° from nadir[1]. These settings yielded points with an average native density of 4.5 points per square meter. The native pulse density is the number of pulses emitted by the LiDAR system from the aircraft. Some types of surfaces (i.e., dense vegetation or water) may return fewer pulses than the laser originally emitted. To increase laser point accuracy, post-processing clipped the laser swath to 13° from nadir, removing the outer 3° of the swath. Therefore, the delivered density is less than the native density and lightly variable according to distributions of terrain, land cover and water body. The entire area was surveyed with opposing flight line side-lap of ≥50% (≥100% overlap) to reduce laser shadowing and increase surface laser painting. The system allows up to four range measurements per pulse, and all laser returns were processed for the output dataset.

To solve for laser point position, it is vital to have an accurate description of aircraft position and attitude. Aircraft position is described as x, y and z and measured twice per second (2 Hz) by an onboard differential GPS unit. Aircraft attitude is measured 200 times per second (200 Hz) as pitch, roll and yaw (heading) from an onboard inertial measurement unit (IMU).

[1] Nadir refers to the perpendicular vector to the ground directly below the aircraft. Nadir is commonly used to measure the angle from the vector and is referred to a "degrees from nadir".

Throughout each flight of the survey, two dual-frequency DGPS base stations recorded fast static (1 Hz) data near Chehalis and at the western edge of the study area (near Doty). The fast static ground GPS data were then later used to calculate a kinematic correction for the aircraft position.

2.2 Ground Survey – Instrumentation and Methods

During the LiDAR survey, multiple static (1 Hz recording frequency) ground surveys are conducted over monuments with known coordinates. After the airborne survey the static GPS data are processed using the Online Positioning User Service (OPUS[2]) as a check against NGS published coordinates and to quantify daily variance. Multiple sessions were processed over the same monument to confirm antenna height measurements and reported position accuracy. OPUS calculates the positions of base stations using continuously operating reference stations (CORS), a national network of GPS stations from which a triangulated location was calculated. **Table 2** summarizes the base station coordinates used for kinematic post-processing of the aircraft GPS data.

Table 2. Base Station Surveyed Coordinates

Datum	NAD83(CORS96)		GRS80
Base Station ID	Latitude (North)	Longitude (West)	Ellipsoid Height (m)
LC 1	46°37'52.78934"	123°16'30.92680"	77.175
LC 2	46°38'44.41450"	122°58'56.13467"	34.160
LC 3	46°40'23.43445"	122°59'10.58452"	32.092

Multiple Thales Z-max DGPS units are used for the ground real-time kinematic (RTK) portion of the survey. To collect accurate ground surveyed points, a GPS base unit is set up over a known monument to broadcast a kinematic correction to a roving GPS unit. The ground crew uses a roving unit to receive radio-relayed kinematic corrected positions from the base unit. This method is referred to as real-time kinematic (RTK) surveying and allows precise location measurement ($\sigma \leq 1.5$ cm ~ 0.6 in). Over 1,500 RTK ground points were collected throughout the study area.

[2] Online Positioning User Service (OPUS) is run by the National Geodetic Survey to process corrected monument positions.

Figure 3. Locations of utilized monuments and RTK survey points. Three base station locations were used during the surveys, with at least two active per flight. Ground surveys collected 1,522 RTK points throughout the study area.

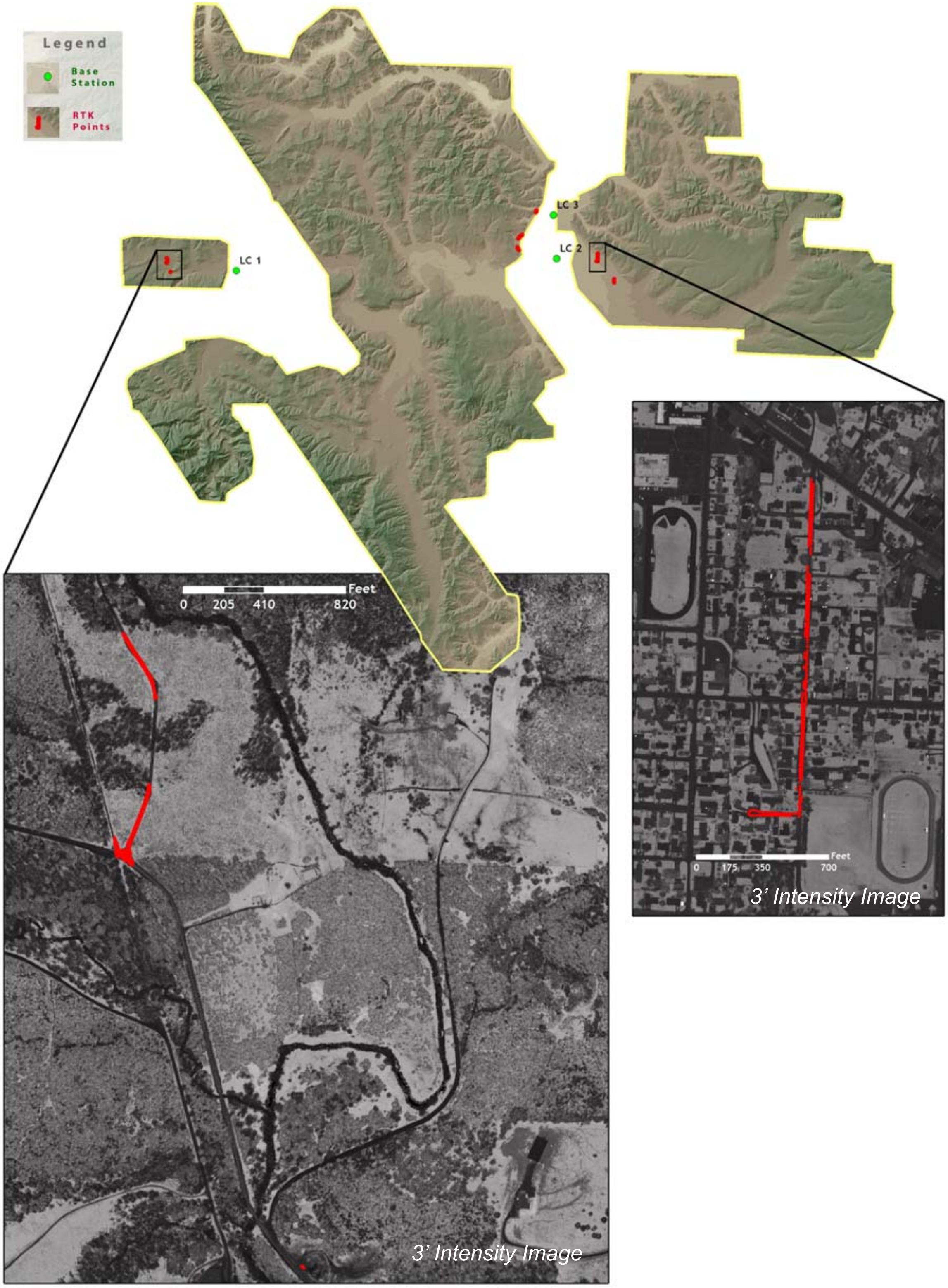

3. LiDAR Data Processing

3.1 Applications and Work Flow Overview

1. Resolve kinematic corrections for aircraft position data using kinematic aircraft GPS and static ground GPS data.
   Software: POSPac v4.2, Module: POSGPS
2. Develop a smoothed best estimate of trajectory (SBET) file that blends the post-processed aircraft position with attitude data. Sensor head position and attitude are calculated throughout the survey. The SBET data are used extensively for laser point processing.
   Software: POSPac v4.2, Module: POSProc
3. Calculate laser point position by associating the SBET position to each laser point return time, scan angle, intensity, etc. Creates raw laser point cloud data for the entire survey in *.las format.
   Software: REALM v3.5.2
4. Import raw laser points into manageable blocks (less than 500 MB) to perform manual relative accuracy calibration and filter for pits/birds. Ground points are then classified for individual flight lines (to be used for relative accuracy testing and calibration).
   Software: TerraScan v.6.008
5. The relative accuracy is tested using ground classified points per each flight line. Automated line to line calibrations are then performed for system attitude parameters (pitch, roll, heading), mirror flex (scale) and GPS/IMU drift. Calibrations are performed on ground classified points from paired flight lines. Every flight line is used for relative accuracy calibration, in this case, utilizing over 1 billion laser points. The final relative accuracy is calculated for each line and summarized for each Julian day and for the entire survey (see **Figure 5**).
   Software: TerraMatch v.6.005
6. Position and attitude data are imported and used to cut the flight line swath to a maximum of $\pm 13^{o}$ from nadir. Resulting data are classified as ground and non-ground points. Statistical absolute accuracy is assessed via direct comparisons of ground classified points to ground RTK survey data. Data are then converted to orthometric (NAVD88) by applying a Geoid03 correction. Ground models are created as a triangulated surface and exported as ArcInfo ASCII grids. Highest hit surfaces are developed from all points and exported as ArcInfo ASCII grids. Intensity images (GeoTIFF format) are created with averages of the laser footprint. All raster data are mosaicked to the 7.5 minute quad delineation.
   Software: TerraScan v.6.008, Fusion v2.1, ArcMap v9.1
7. Contours are developed from TINs derived from ground points as AutoCAD drawing format, and converted to ESRI vector data.
   Software: TerraModeler v.6.004, ArcMap v9.1
8. The $1/64^{th}$ quad delineated LAS files (ASPRS v1.0) are converted to ASCII format, preserving all LAS fields.
   Software: Custom

3.2 Aircraft Kinematic GPS and IMU Data

LiDAR survey datasets are referenced to 1 Hz static ground GPS data collected over pre-surveyed monuments with known coordinates. While surveying, the aircraft collects 2 Hz kinematic GPS data. The onboard inertial measurement unit (IMU) collects 200 Hz aircraft attitude data. POSGPS v4.2 is used to process the kinematic corrections for the aircraft. The static and kinematic GPS data are then post-processed after the survey to obtain accurate GPS solution and aircraft positions. POSProc v4.2 is used to develop a trajectory file that includes corrected aircraft position and attitude information. The trajectory data for the entire flight survey session are incorporated into a final smoothed best estimate trajectory (SBET) file that contains accurate and continuous aircraft positions and attitudes.

3.3 Laser Point Processing

Laser point coordinates are computed using the REALM v. 3.5.2 software suite based on independent data from the LiDAR system (pulse time, scan angle), and aircraft trajectory data (SBET). Laser point returns (first through fourth) are assigned an associated (x, y, z) coordinate, along with unique intensity values (0-255). The data are output into large LAS v. 1.0 files; each point maintains the corresponding scan angle, return number (echo), intensity, and x, y, z (easting, northing, and elevation) information.

These initial laser point files are too large to process (i.e. > 40 GB). To facilitate laser point processing, bins (polygons) are created to divide the dataset into manageable sizes (less than 500 MB). The study area is divided into individual bins, approximately 1 km^2 each; these are ultimately aggregated into areas of 0.9375-minute quadrangles (1/64^{th} of a standard USGS 7.5-minute quadrangle). Flight lines and LiDAR data are then reviewed to ensure complete coverage of the study area and positional accuracy of the laser points.

Once the laser point data are imported into bins in TerraScan, a manual calibration is performed to assess the system offsets for pitch, roll, heading and mirror scale. Using a geometric relationship developed by Watershed Sciences, each of these offsets is resolved and corrected if necessary.

The LiDAR points are then filtered for noise, pits and birds by screening for absolute elevation limits, isolated points and height above ground. Each bin is then inspected for pits and birds manually; spurious points are removed. For a bin measuring 1 km^2, an average of 20-40 points are typically found to be artificially low or high.

Spurious non-terrestrial laser points must be removed from the dataset. Common sources of non-terrestrial returns are clouds, birds, vapor and haze. Additionally, rare and unique features such as a factory with visible emissions require the removal of the smoke from the LiDAR point cloud during post-processing (see **Figure 4)**.

Figure 4. Spurious, non-terrestrial laser points must be removed from the dataset, such as smoke emissions as shown here, which results in decreased point density. This site is 8 miles northeast of Centralia.

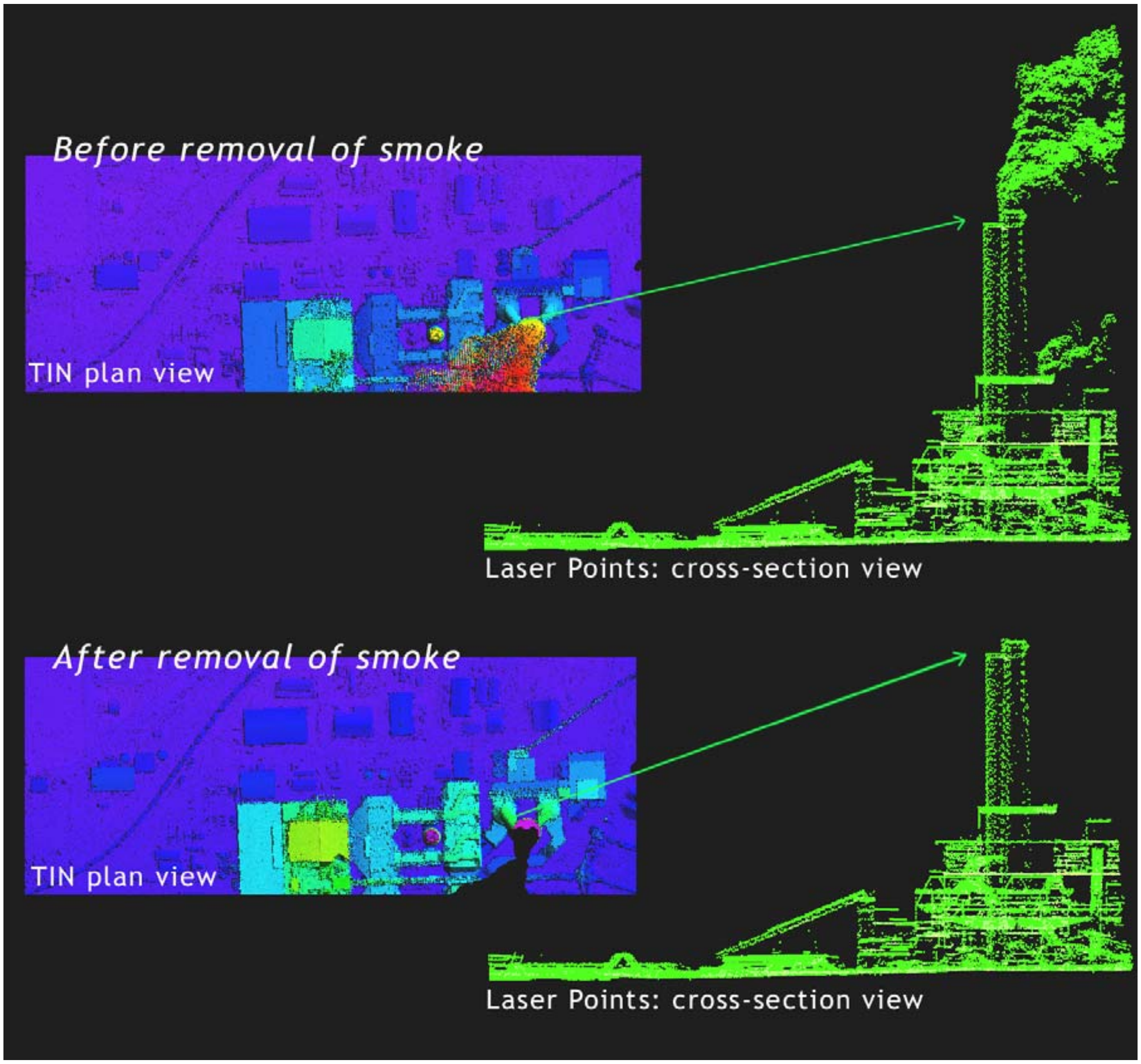

The internal calibration is refined using TerraMatch. Points from overlapping lines are tested for internal consistency and final adjustments are made for system misalignments (i.e., pitch, roll, heading offsets and mirror scale). Automated sensor attitude and scale corrections yield 3-5 cm improvements in the relative accuracy. Once the system misalignments are corrected, vertical GPS drift is then resolved and removed per flight line, yielding a slight improvement (<1 cm) in relative accuracy. The resulting dataset is deemed internally calibrated to a relative accuracy of 8.1 cm at one sigma (1σ) based on over 1.4 billion point to point comparisons from overlapping flight lines. At this point in the workflow, data have passed a robust calibration designed to reduce inconsistencies from multiple sources (i.e. sensor attitude offsets, mirror scale, GPS drift) using a procedure that is comprehensive (i.e. uses all of the overlapping survey data). Relative accuracy screening is complete.

The TerraScan software suite is designed specifically for classifying near-ground laser points (Soinenen, 2004). The processing sequence begins by 'removing' all points that are not 'near' the earth based geometric constraints used to evaluate multi-return points. The resulting bare earth (ground) model is visually inspected and additional ground point modeling is performed in site-specific areas (over a 50 meter radius) to improve ground detail. This was only done in areas with known ground modeling deficiencies, such as: bedrock outcrops, cliffs, deeply incised stream banks, and dense vegetation. In some cases, ground point classification included known vegetation (i.e., understory, low/dense shrubs, etc.) and these points were reclassified as non-grounds. Ground surface raster and contour vector data are developed from triangulated irregular networks (TINs) of ground points.

Non-ground points are used to create two vegetation surface models. A custom vegetation surface raster is developed using Fusion v.2.1 deforestation algorithms (Haugerud and Harding, 2001; Andersen et al. 2003; McGaughey and Carson, 2003; McGaughey, in progress[3]). A traditional highest hit vegetation surface raster is also created. Paired comparisons of the vegetation models reveal varied differences, although no quantitative analysis is conducted to assess the accuracy of either vegetation surface.

3.4 Laser Point Accuracy

Laser point absolute accuracy is largely a function of internal consistency (measured as relative accuracy) and laser noise:

- **Laser Noise**: For any given target, laser noise is the breadth of the data cloud per laser return (i.e., last, first, etc.). Lower intensity surfaces (roads, rooftops, still/calm water) experience higher laser noise. The laser noise range for this mission varies between 0.04 - 0.05 meters.

- **Relative Accuracy**: Internal consistency refers to the ability to place a laser point in the same location over multiple flight lines, GPS conditions, and aircraft attitudes. <u>The data exhibit a 1σ relative accuracy of 0.081 meters based upon >1.4 billion overlapping flight line point to point comparisons.</u>

- **Absolute Accuracy**: 1,522 RTK GPS measurements were compared to the LiDAR point data. <u>The root mean square error (RMSE) is 0.21 feet, the 1σ absolute deviation is 0.21 feet and the 2σ absolute deviation is 0.42 feet.</u>

[3] McGaughey, *in progress*. Fusion v. 2.1 development and testing.

Table 3. LiDAR accuracy is a combination of several sources of error. These sources of error are cumulative. Some error sources that are biased and act in a patterned displacement can be resolved in post processing.

Type of Error	Source	Post Processing Solution	Effect
GPS (Static/Kinematic)	Long Base Lines	None	
	Poor Satellite Constellation	None	
	Poor Antenna Visibility	Reduce Visibility Mask	Slight
Relative Accuracy	Poor System Calibration	Recalibration IMU and sensor offsets/settings	Large
	Inaccurate System	None	
Laser Noise	Poor Laser Timing	None	
	Poor Laser Reception	None	
	Poor Laser Power	None	
	Irregular Laser Shape	None	

3.4.1 Relative Accuracy

Relative accuracy refers to the internal consistency of the dataset and is measured as the divergence between points from different flight lines within an overlapping area. Divergence is most apparent when flight lines are opposing. When the LiDAR system is well calibrated the line-to-line divergence is low (<10 cm). Internal consistency is affected by system attitude offsets (pitch, roll and heading), mirror flex (scale), and GPS/IMU drift.

Operational measures taken to improve relative accuracy:

1. Low Flight Altitude: Terrain following was targeted at 1200 meters above ground level (AGL) flight altitude. Laser horizontal errors are a function of flight altitude above ground (i.e., ~ 1/3000th AGL flight altitude). Lower flight altitudes decrease laser noise on surfaces with even the slightest relief.
2. Focus Laser Power at narrow beam footprint: A laser return must be received by the system above a power threshold to accurately record a measurement. The strength of the laser return is a function of laser emission power, laser footprint, flight altitude and the reflectivity of the target. While surface reflectivity cannot be controlled, laser power can be increased and low flight altitudes can be maintained.
3. Reduced Scan Angle: Edge-of-scan data can become inaccurate. The scan angle was reduced to a maximum of ±13^{o} from nadir, creating a narrow swath width and greatly reducing laser shadows from trees and buildings.
4. Quality GPS: Flights took place during optimal GPS conditions (e.g., 6 or more satellites and PDOP less than 3.0). Before each flight, the PDOP (Position Dilution of Precision) was determined for the survey day. During all flight times, two (2) dual frequency DGPS base stations recording at 1–second epochs were utilized and a maximum baseline length between the aircraft and the control points was less than 32 kilometers (19.9 miles) at all times.
5. Ground Survey: Ground survey point accuracy (i.e., <1.5 cm RMSE) occurs during optimal PDOP ranges and targets a minimal baseline distance of 4 miles between GPS rover and base. Robust statistics are, in part, a function of sample size (n) and distribution. The ground survey collected 1,522 RTK points well distributed throughout multiple flight lines.
6. 50% Side-Lap (100% Overlap): Overlapping areas are optimized for relative accuracy testing. Laser shadowing is minimized to help increase target acquisition from multiple scan angles. Ideally, with a 50% side-lap, the most nadir portion of one flight line coincides with the edge (least nadir) portion of overlapping flight lines. A minimum of 50% side-lap with terrain-followed acquisition prevents data gaps.
7. Opposing Flight Lines: All overlapping flight lines are opposing. Pitch, roll and heading errors are amplified by a factor of two relative to the adjacent flight line(s), making misalignments easier to detect and resolve.

Relative Accuracy Calibration Methodology

1. Manual System Calibration: Calibration procedures for each mission require solving geometric relationships that relate measured swath-to-swath deviations to misalignments of system attitude parameters. Corrected scale, pitch, roll and heading offsets are calculated and applied to resolve misalignments. The raw divergence between lines is computed after the manual calibration is completed and reported as 1σ of 10.9 cm (see **Figure 5**).

2. Automated Attitude Calibration: All data are tested and calibrated using TerraMatch automated sampling routines. Ground points are classified for each individual flight line and used for line-to-line testing. The resulting overlapping ground points (per line) total over 1.4 billion points from which to compute and refine relative accuracy. System misalignment offsets (pitch, roll and heading) and mirror scale are solved for each individual mission. The application of attitude misalignment offsets (and mirror scale) occurs for each individual mission. After the automated attitude calibration was completed the resulting relative accuracy was a 1σ of 8.8 cm. The data from each mission are then blended when imported together to form the entire area of interest.

3. Automated Z Calibration: Ground points per line are utilized to calculate the vertical divergence between lines caused by vertical GPS drift. The corrections create a slight improvement and the resulting relative accuracy is a 1σ of 8.1 cm. Automated Z calibration is the final step employed for relative accuracy calibration.

Figure 5. Deviation per line reported for each Julian day and all data reported as 1σ.

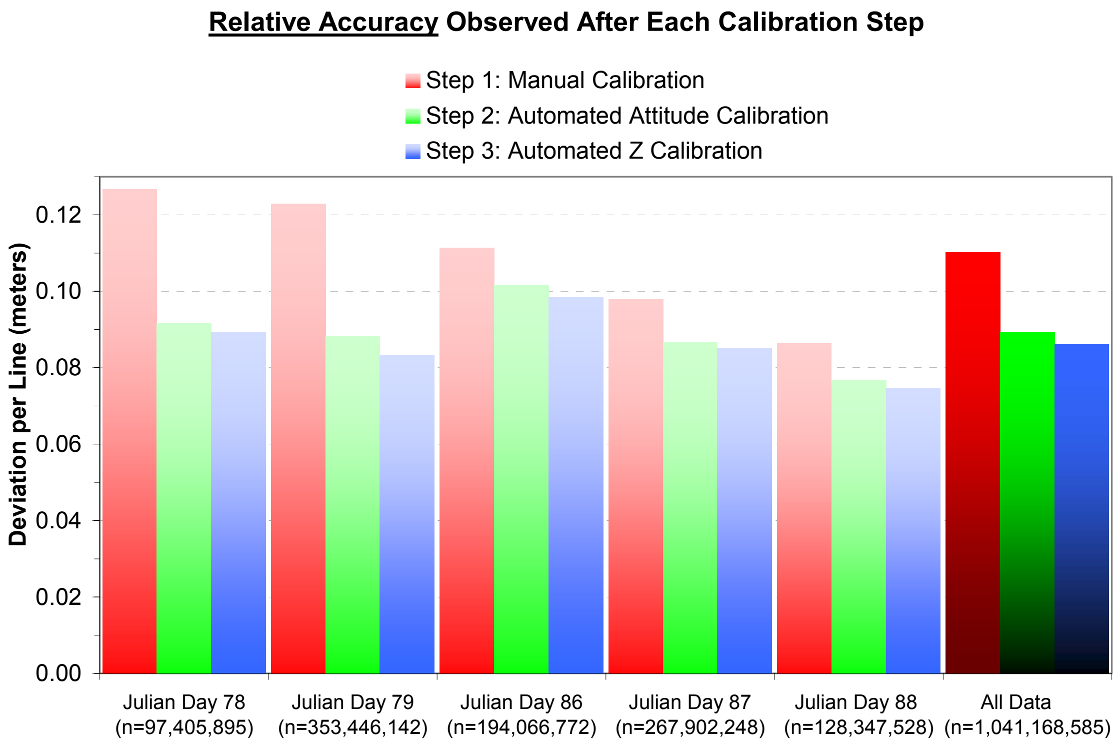

3.4.2 Absolute Accuracy

The final quality control measure is a statistical accuracy assessment that compares known RTK ground survey points to the closest laser point. Accuracy statistics are reported in **Table 4** and shown in **Figures 6** and **7**.

Table 4. Absolute Accuracy – Deviation between laser points and RTK survey points.

Sample Size (n): 1,522	
Root Mean Square Error (RMSE): 0.21 feet	
Standard Deviations	**Deviations**
1 sigma (σ): 0.20 feet	**Minimum Δz:** -0.85 feet
2 sigma (σ): 0.42 feet	**Maximum Δz:** 0.68 feet
	Average Δz: 0.00 feet

Figure 6. Point Deviation Statistics

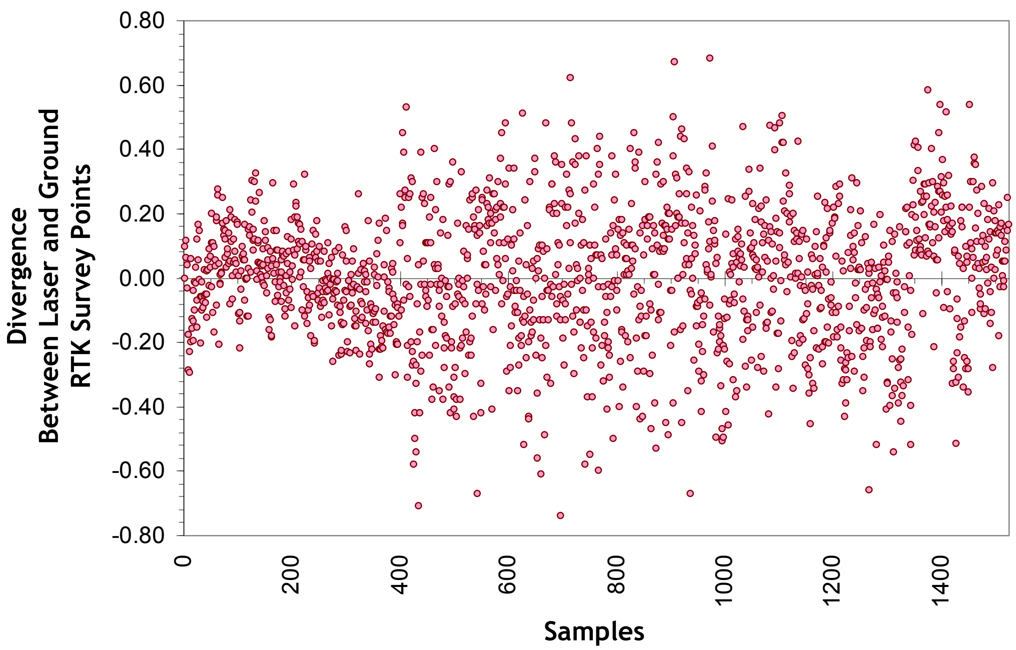

Figure 7. Point Absolute Deviation Statistics

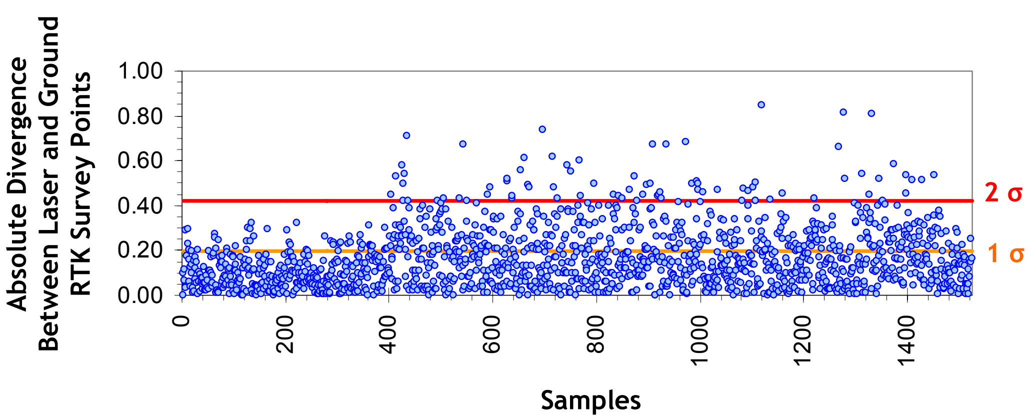

3.5 Datum and Projection

The data were processed as ellipsoidal elevations and required a Geoid transformation to convert the elevations into orthometric (NAVD88). In TerraScan, the NGS published Geiod03 model is applied to each point. The data are processed with U.S. survey feet units in the Washington State Plane South Coordinate System FIPS 4602 and NAD83(CORS96)/NAVD88 datum.

4. Deliverables

4.1 Point Data (per 0.9375-minute quadrangle ~ 1/64th Quads)

Data Fields: Number, X, Y, Z, Intensity, ReturnNumber, NumReturns, ScanDirection, EdgeOfFlightLine, Class, ScanAngleRank, FileMarker, UserBitField, GPSTime

- ASCII space delimited
  - All Points (*.txt)
  - Ground Points (*.gnd)

4.2 Raster Data (per 7.5-minute quadrangle)

- ESRI GRIDs of LiDAR dataset:
  - Bare Earth Modeled Points (3-foot and 6-foot resolution),
  - Vegetation Modeled Points- Highest Hit model (3-foot resolution),
  - Vegetation Modeled Points- Fusion 5x5 v.2.1 model (3-foot resolution),
- Surface intensity images in GEOTIFF format (3-foot resolution),

4.3 Vector Data

- 2-foot Contour Data (per 0.9375-minute quadrangle ~ 1/64th Quads)
  - AutoCAD Format (*.dwg)
  - Shapefile format
- Areas of Interest in shapefile format
- Total Area Flown
  - 7.5-minute quadrangle delineation in shapefile format
  - 0.9375-minute quadrangle delineation in shapefile format

4.4 Data Report

- Full Report containing introduction, methodology, accuracy, and examples
  - Word Format (*.doc)
  - PDF Format (*.pdf)

Raster data are delivered according to standard USGS 7.5-minute quadrangle boundaries. Point and contour deliverables are in 0.9375-minute quadrangles (64 units per 7.5-minute quadrangle). **Figure 8** shows the 7.5-minute quadrangle boundaries for the study area. **Figure 9** on the following page describes the naming convention used for the 0.9375-minute quadrangle deliverables.

Figure 8. 7.5-Minute and 0.9375-Minute Quadrangle Boundaries.

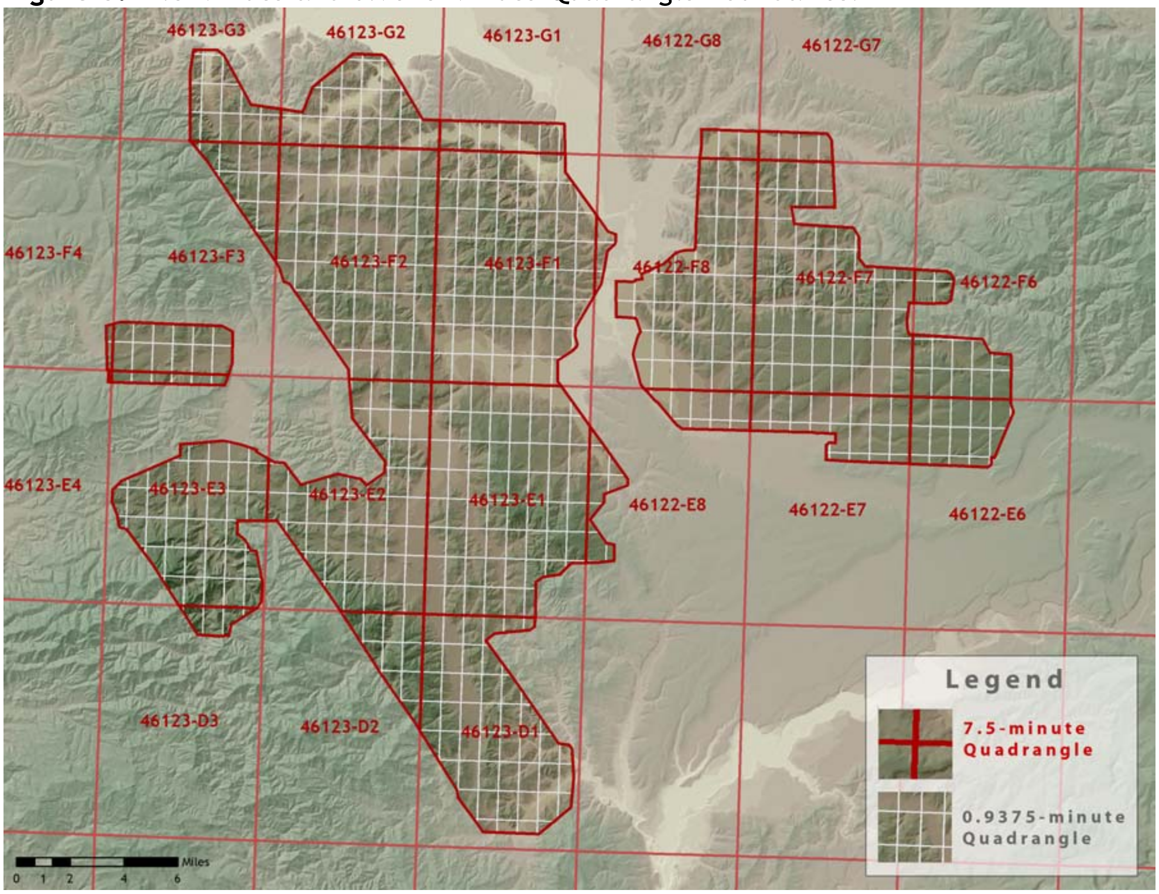

Figure 9. Naming convention for the 7.5-minute to 0.9375-minute quadrangles. Each time a quadrangle is quartered, the nomenclature begins in the upper right quadrant and progresses counter-clockwise.

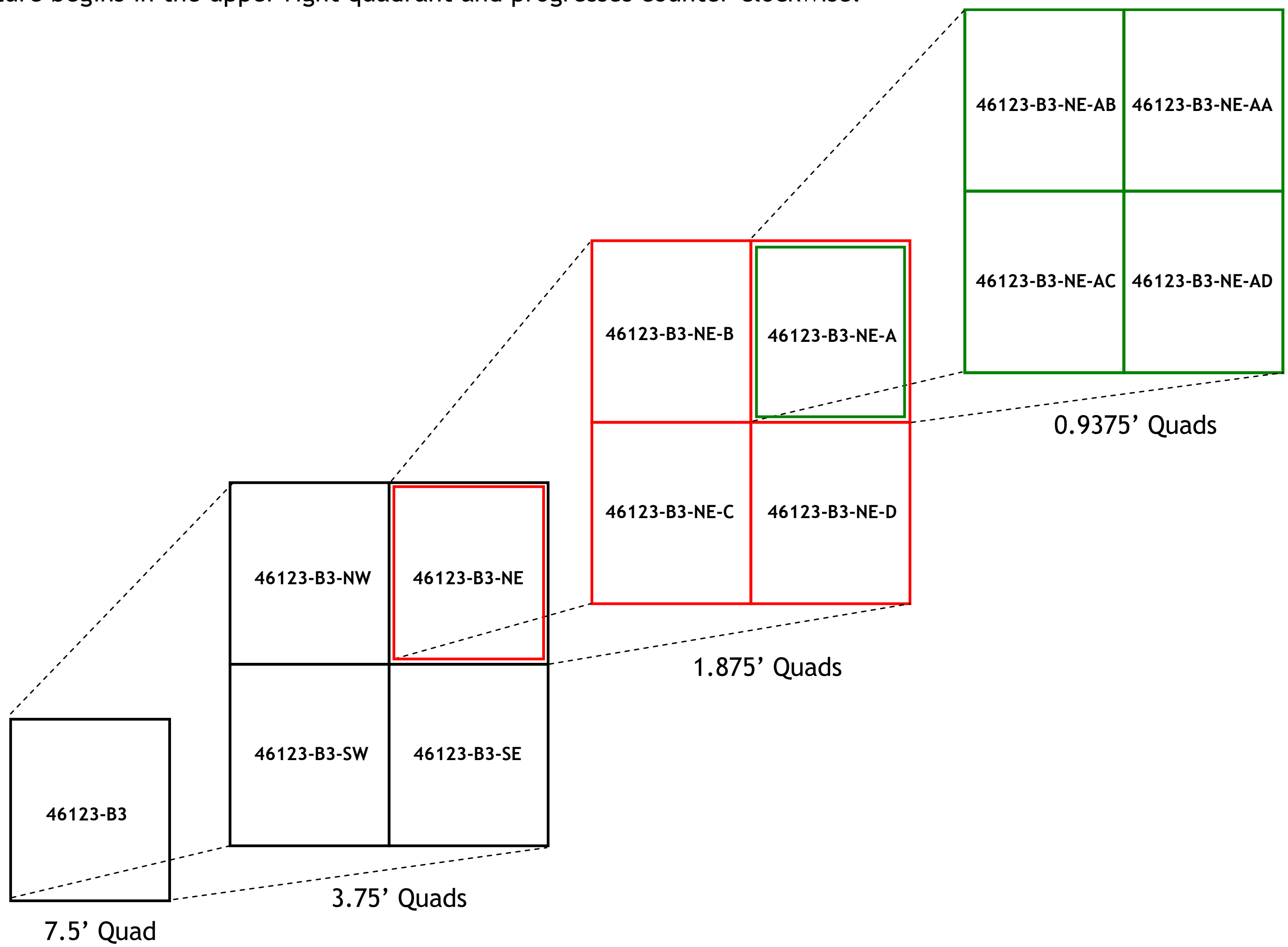

5. Selected Images ~ Examples of Paired Datasets

5.1 Plan View Data

The example areas are presented to show the following plan view datasets (see **Figures 10** through **18**):

- Bare earth 3’ pixel resolution ESRI Grids,
- 2’ Contours over the corresponding bare earth 3’ pixel resolution ESRI Grids,
- Highest hit 3’ pixel resolution ESRI Grids,
- Fusion vegetation 3’ pixel resolution ESRI Grids, and
- Intensity image 3’ pixel GeoTIFF

5.2 Three Dimensional Oblique View Data Pairs

The example areas are presented to show paired 3-d oblique view imagery (see **Figures 19** through **29**):

- Elevation colored bare earth raster with ½-foot pixel resolution, and
- Elevation colored laser point cloud with intensity shading over the bare earth raster with ½-foot pixel resolution.

Figure 10. Bare Earth Raster and 2' Contours (Example Area 1)

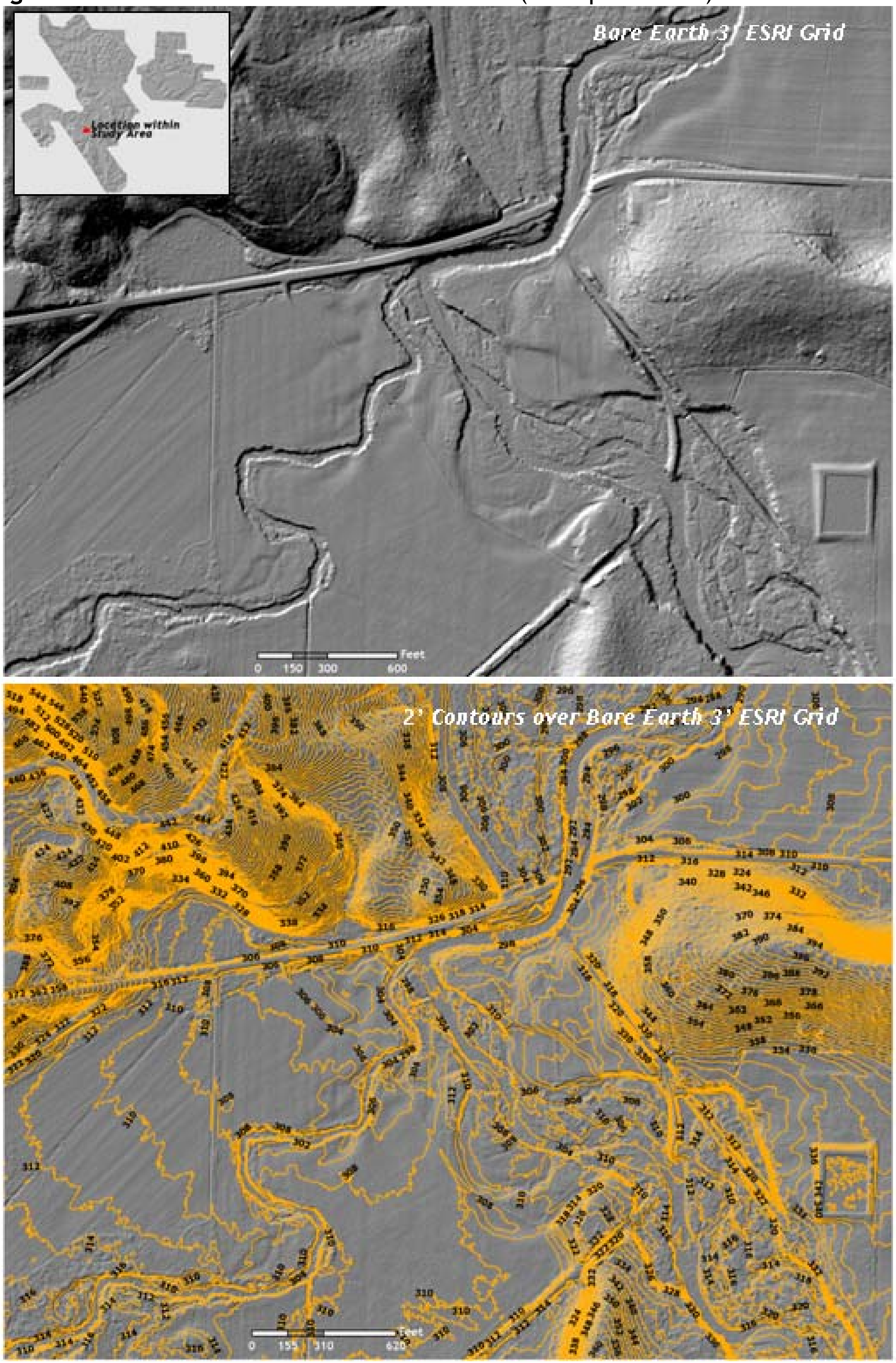

Figure 11. Highest Hits and Fusion Vegetation Rasters (Example Area 1)

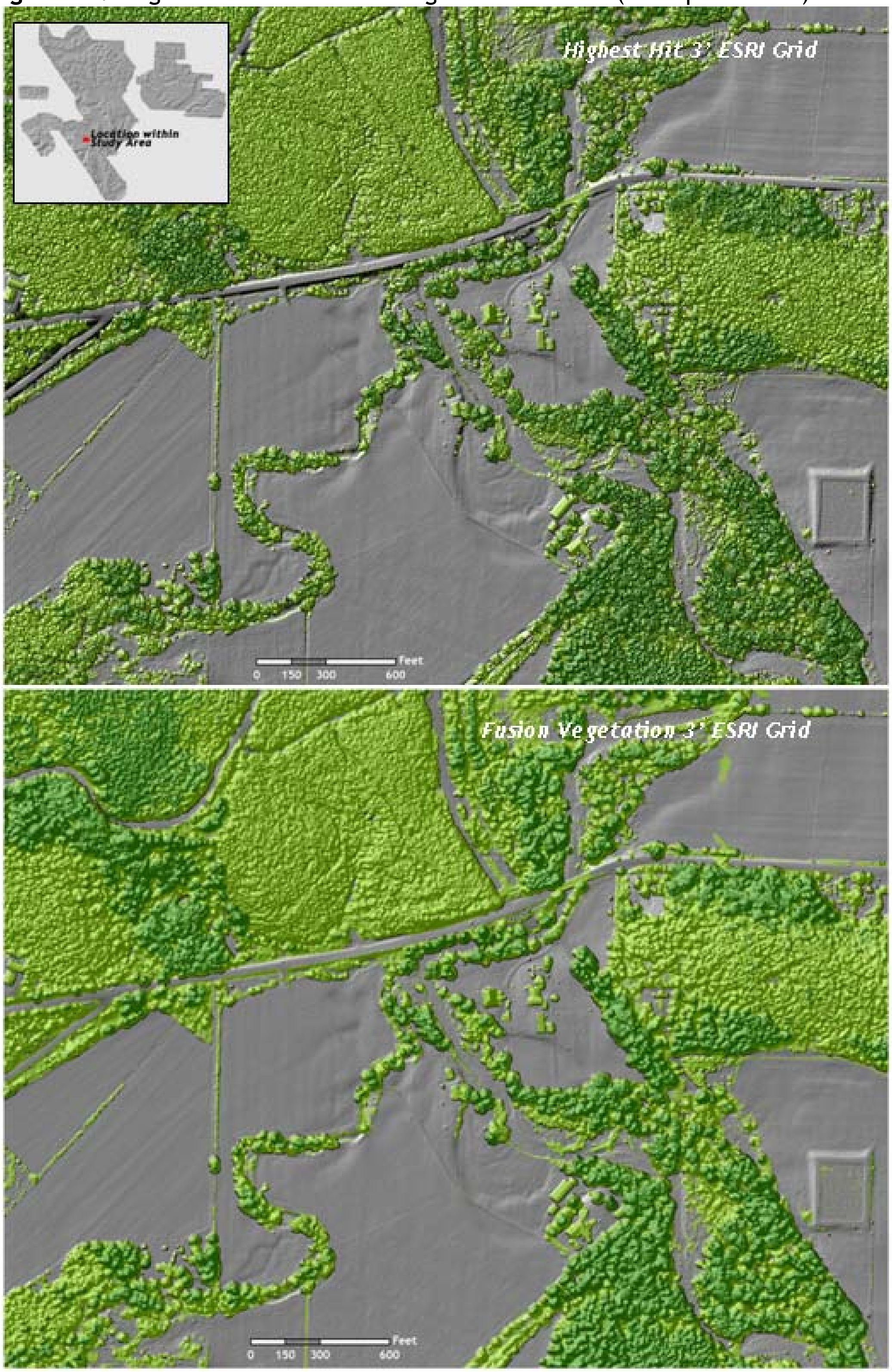

Figure 12. Intensity GeoTIFF (Example Area 1)

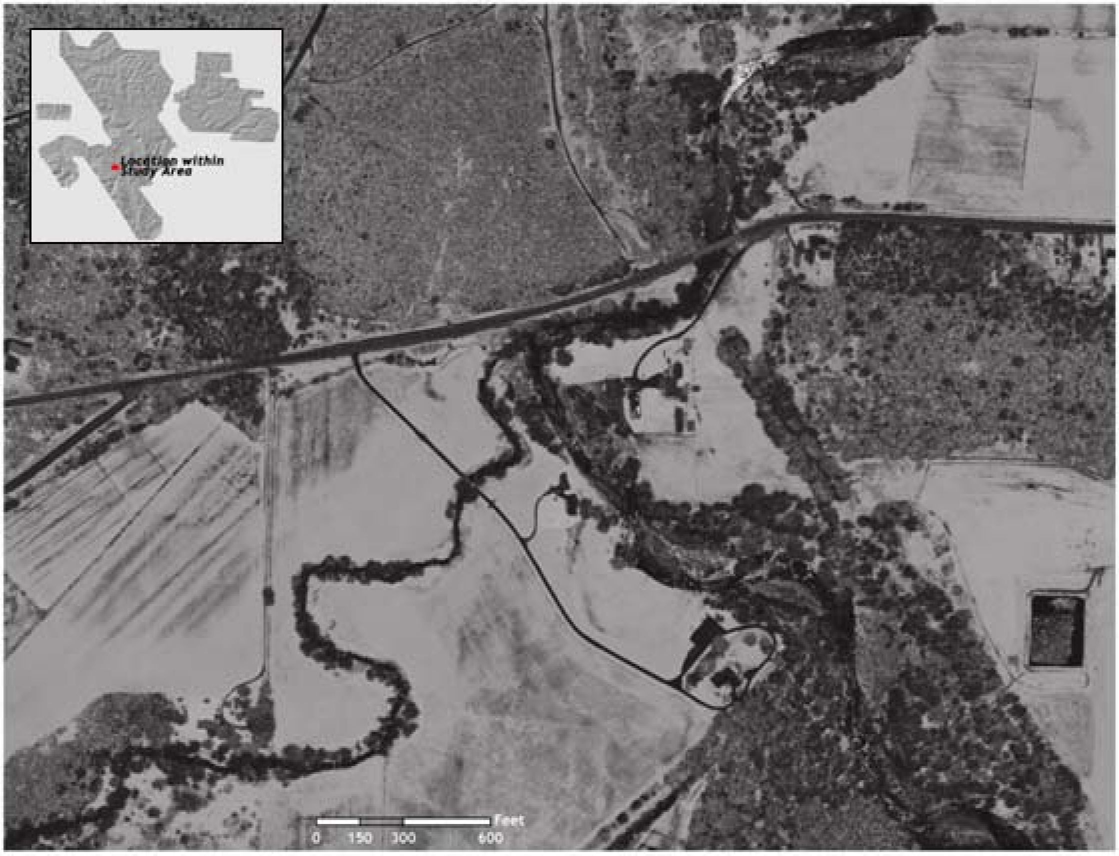

Figure 13. Bare Earth Data Raster and 2' Contours (Example Area 2)

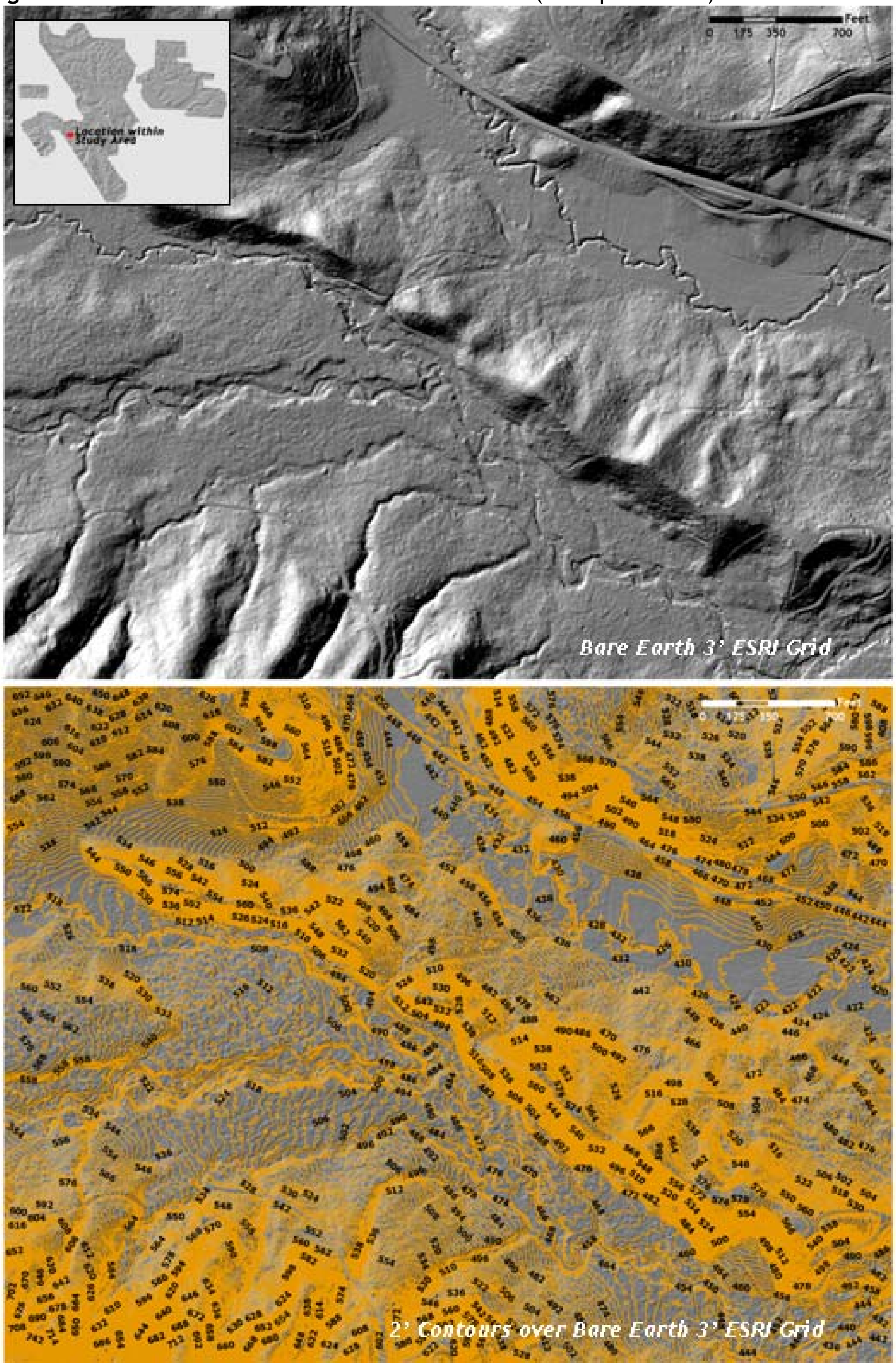

Figure 14. Highest Hits and Fusion Vegetation Rasters (Example Area 2)

Figure 15. Intensity GeoTIFF (Example Area 2)

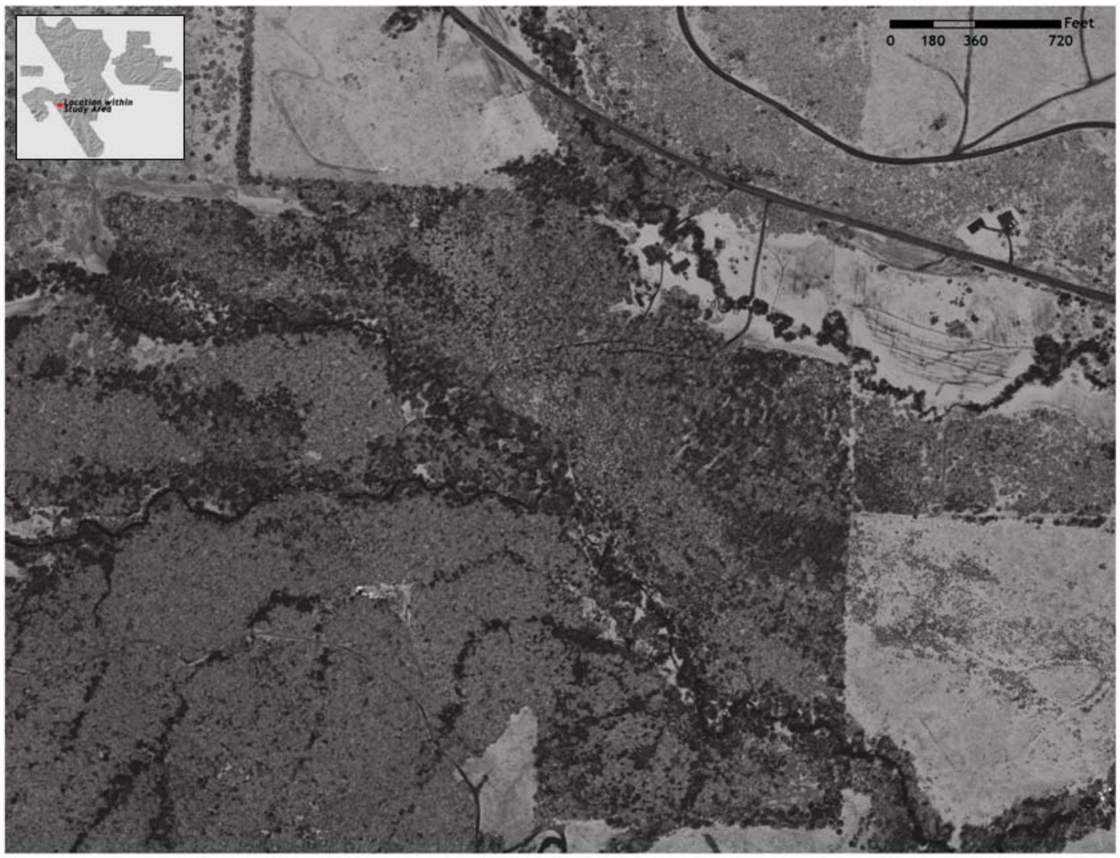

Figure 16. Bare Earth Raster and 2' Contours (Example Area 3)

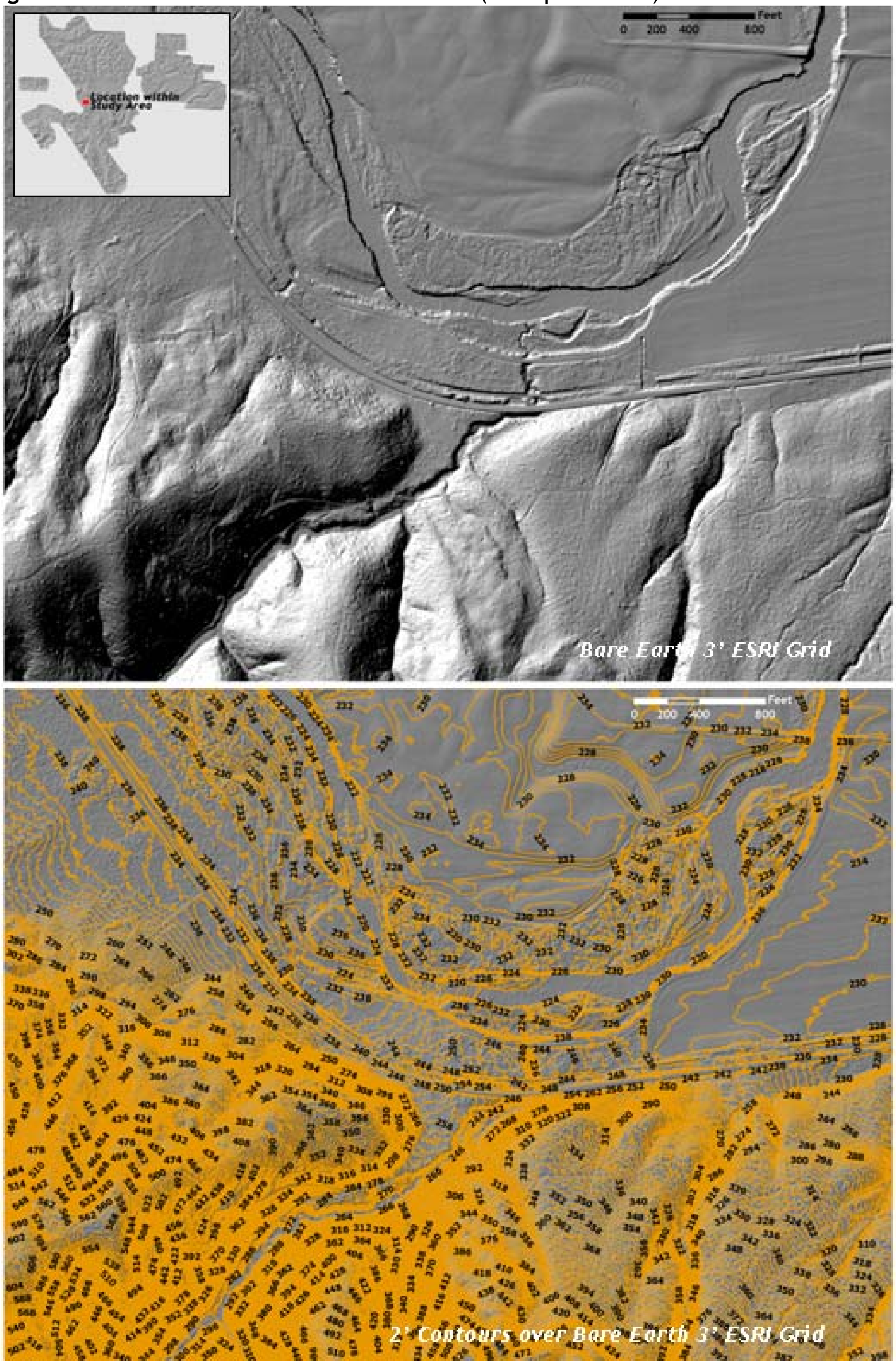

Figure 17. Highest Hits and Fusion Vegetation Rasters (Example Area 3)

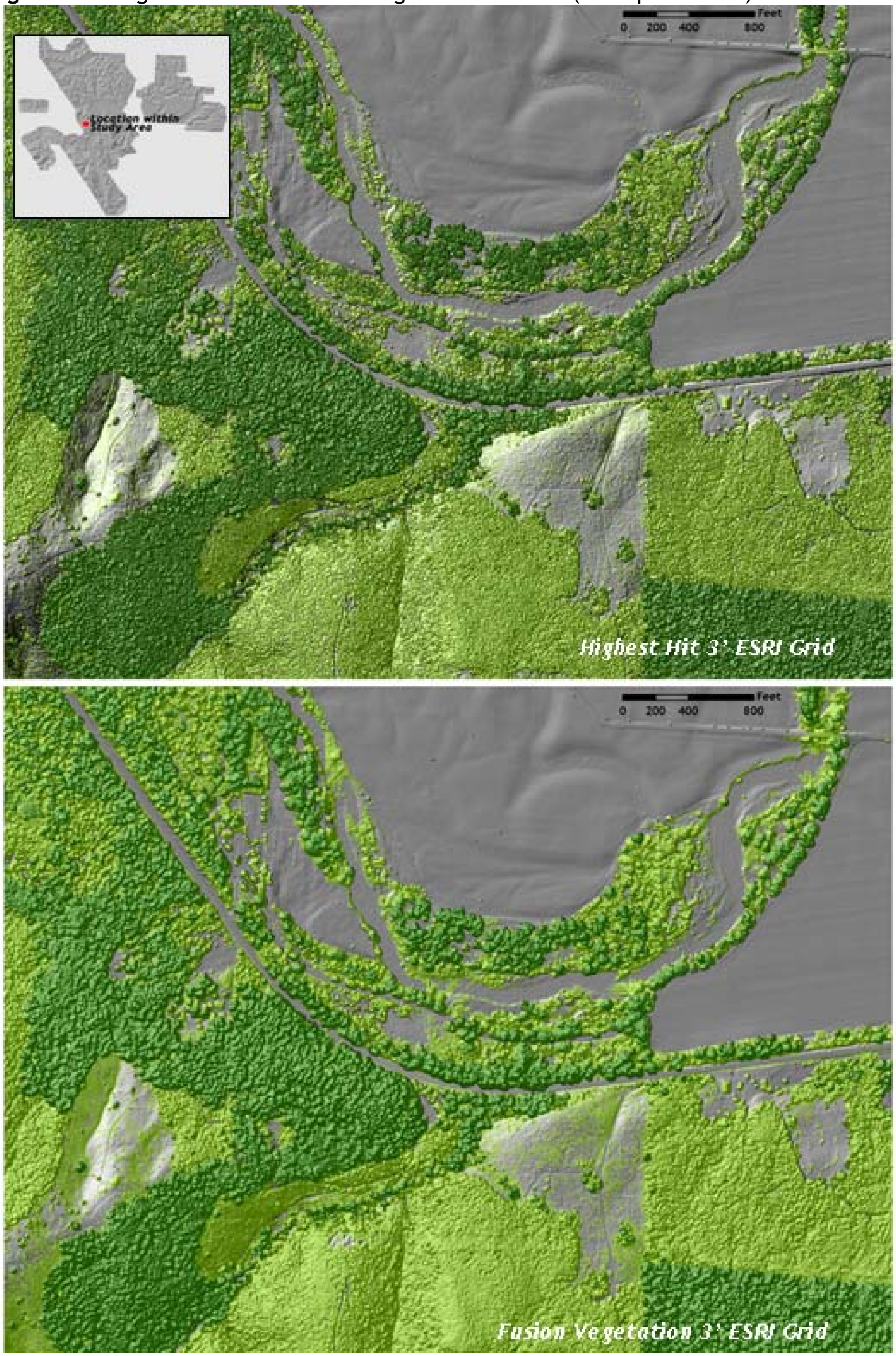

Figure 18. Intensity GeoTIFF (Example Area 3)

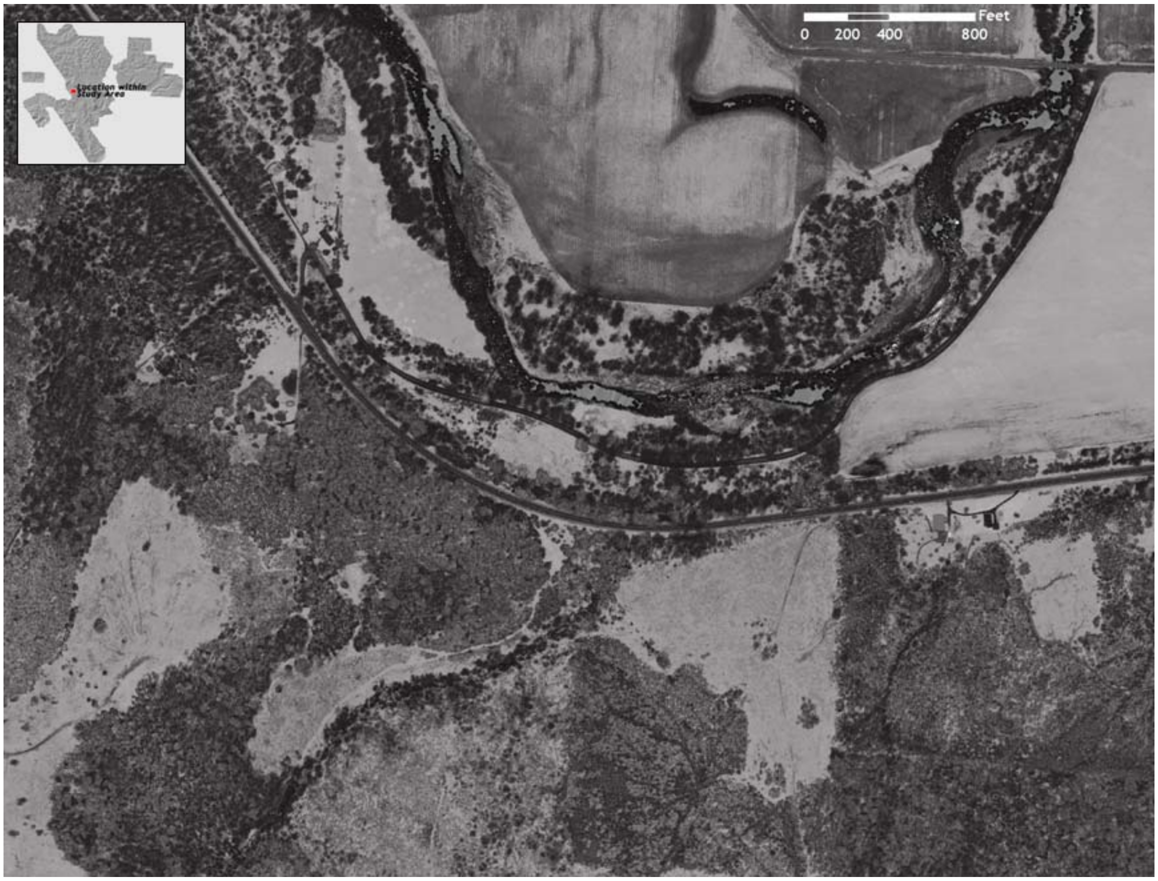

Figure 19. Paired 3-d oblique images of 46122-e6-nw-bb (above: elevation-colored, 0.5-foot resolution bare earth raster; below: elevation-colored laser point cloud with intensity shading over the bare earth raster)

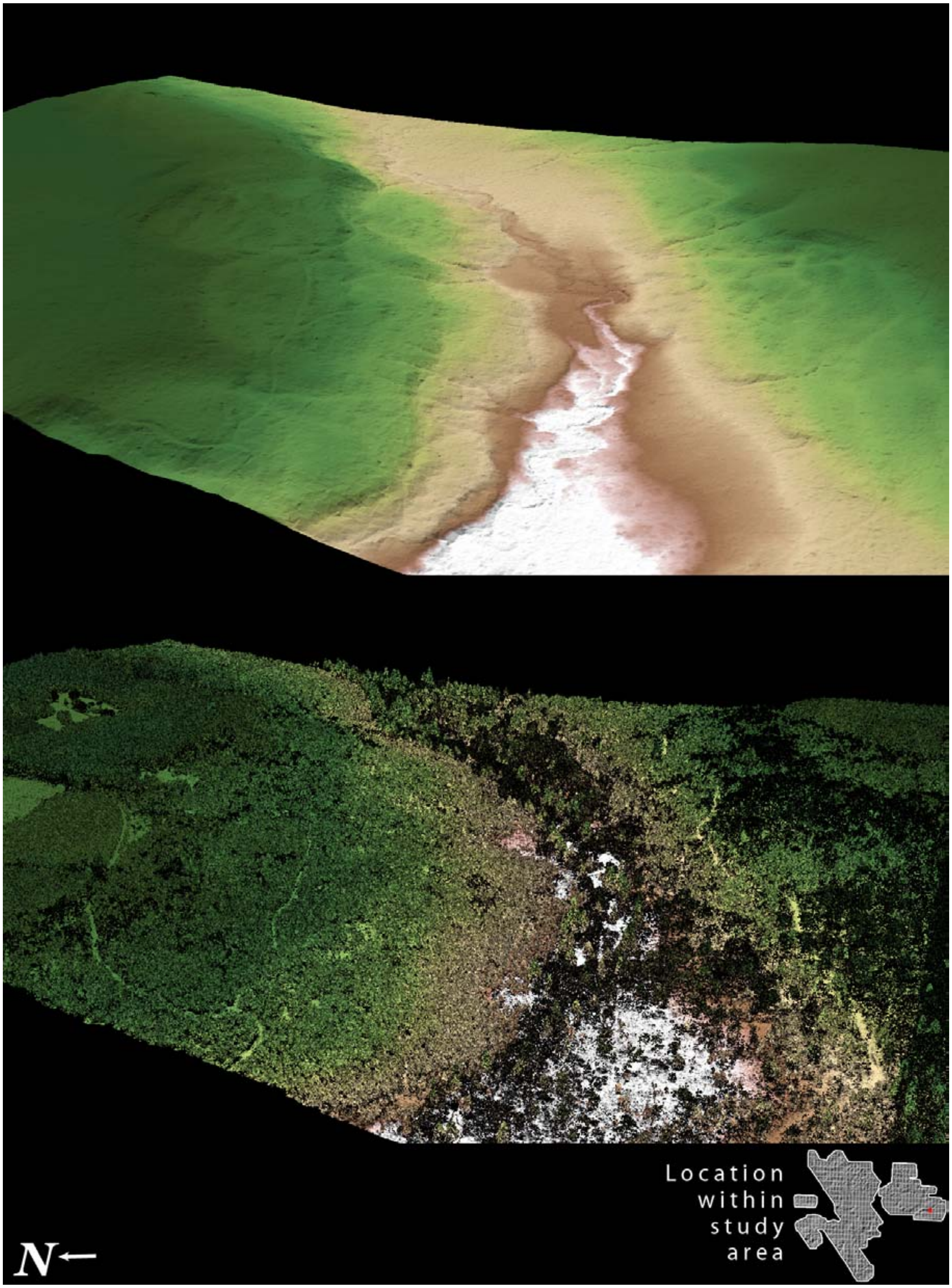

Figure 20. Paired 3-d oblique images of 46122-f7-sw-bb (above: elevation-colored, 0.5-foot resolution bare earth raster; below: elevation-colored laser point cloud with intensity shading over the bare earth raster)

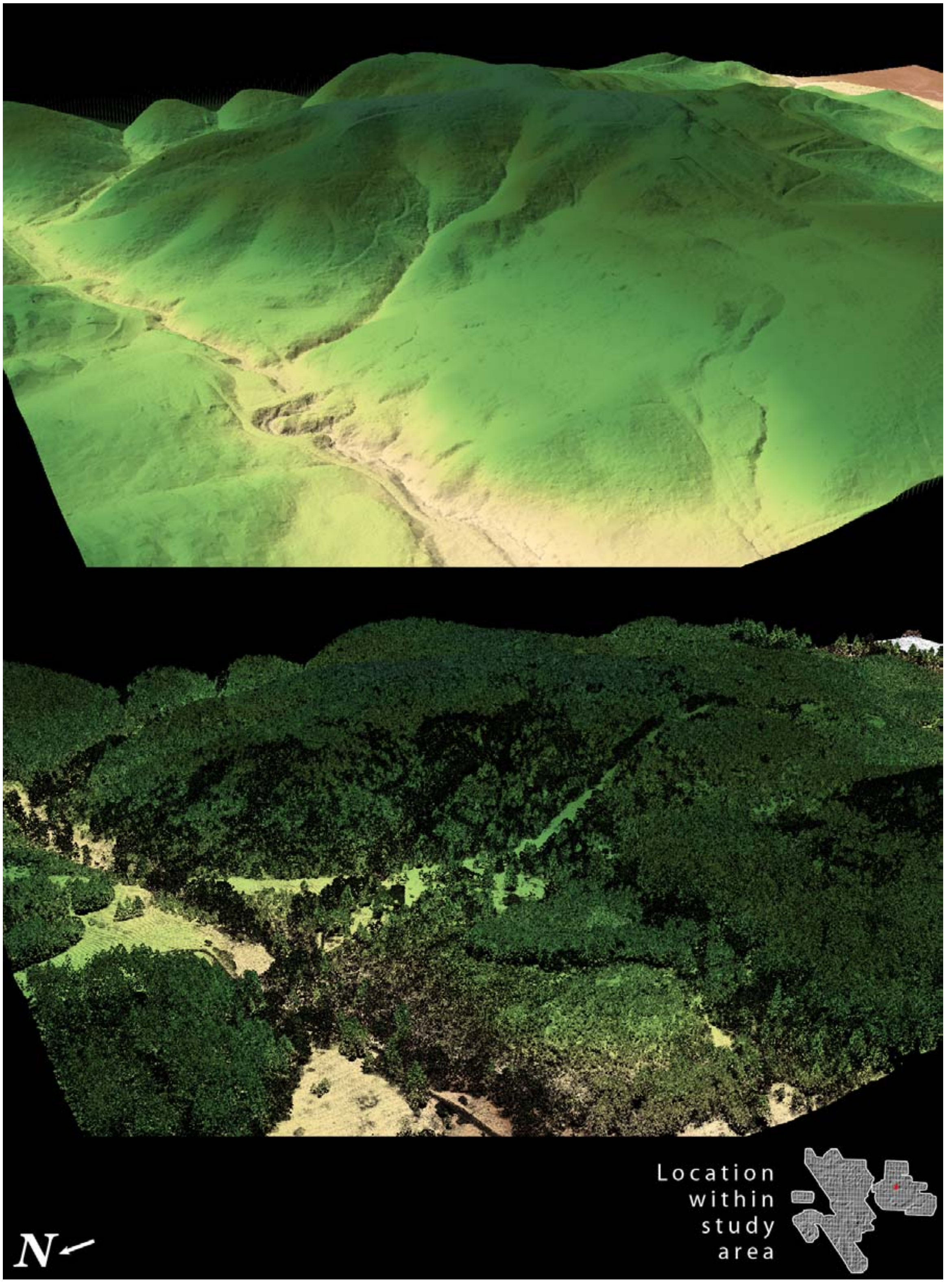

Figure 21. Paired 3-d oblique images of 46122-f8-sw-da (above: elevation-colored, 0.5-foot resolution bare earth raster; below: elevation-colored laser point cloud with intensity shading over the bare earth raster)

Figure 22. Paired 3-d oblique images of 46123-d1-se-ac (above: elevation-colored, 0.5-foot resolution bare earth raster; below: elevation-colored laser point cloud with intensity shading over the bare earth raster)

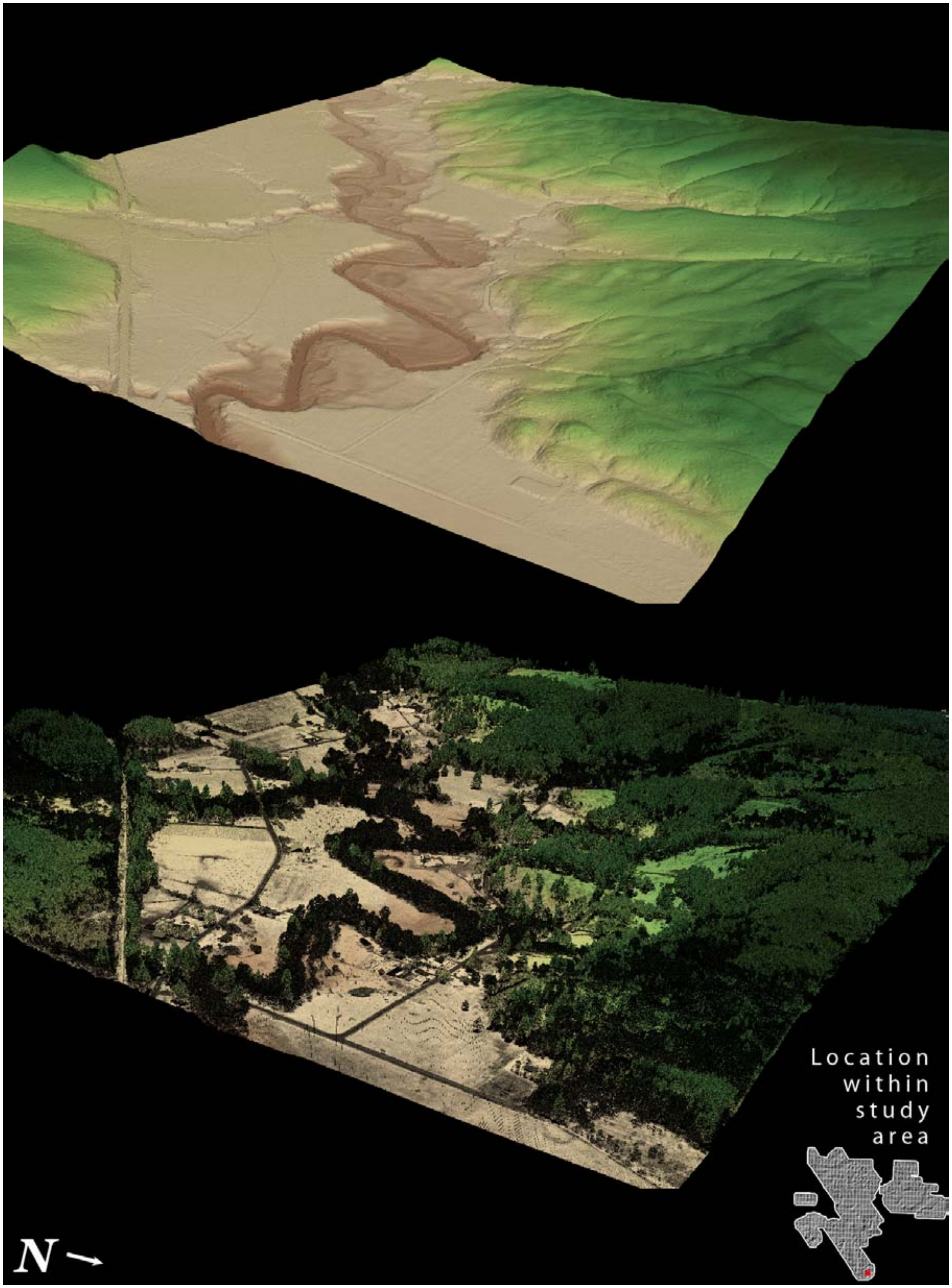

Figure 23. Paired 3-d oblique images of 46123-e1-nw-bc (above: elevation-colored, 0.5-foot resolution bare earth raster; below: elevation-colored laser point cloud with intensity shading over the bare earth raster)

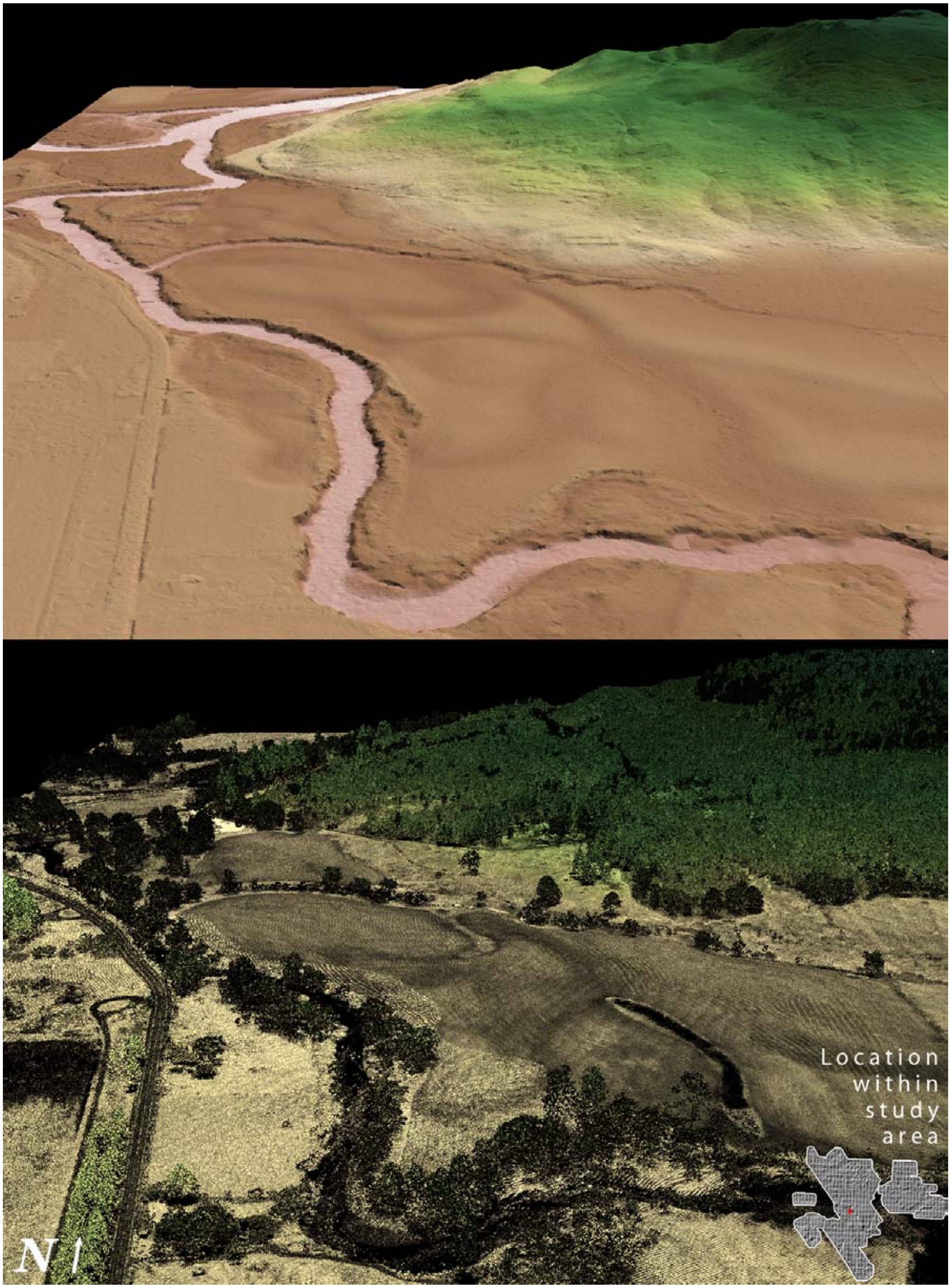

Figure 24. Paired 3-d oblique images of 46123-f1-nw-ab (above: elevation-colored, 0.5-foot resolution bare earth raster; below: elevation-colored laser point cloud with intensity shading over the bare earth raster)

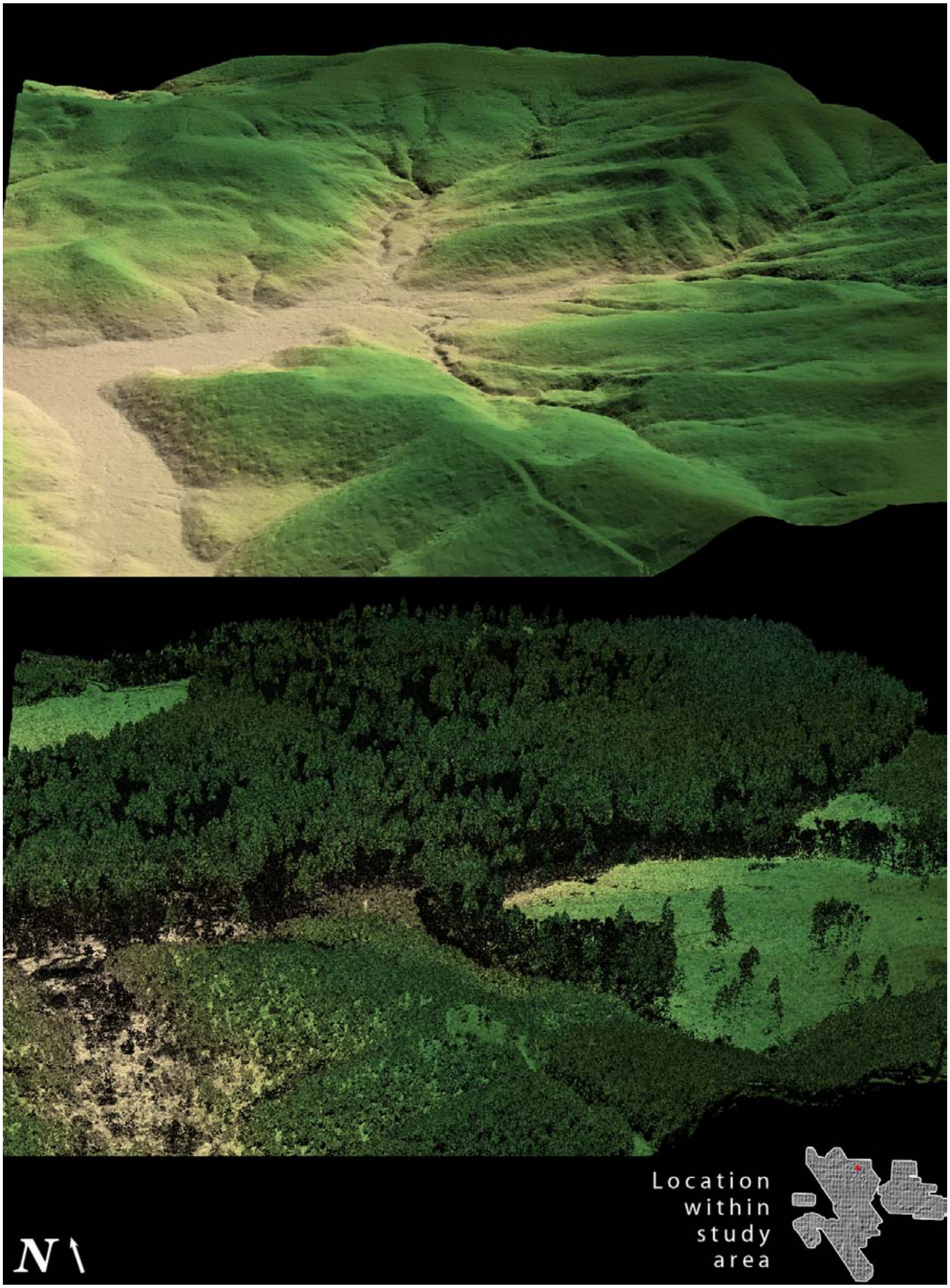

Figure 25. Paired 3-d oblique images of 46123-f2-nw-bb (above: elevation-colored, 0.5-foot resolution bare earth raster; below: elevation-colored laser point cloud with intensity shading over the bare earth raster)

Figure 26. Paired 3-d oblique images of 46123-f2-sw-ac (scene 1) (above: elevation-colored, 0.5-foot resolution bare earth raster; below: elevation-colored laser point cloud with intensity shading over the bare earth raster)

Figure 27. Paired 3-d oblique images of 46123-f2-sw-ac (scene 2) (above: elevation-colored, 0.5-foot resolution bare earth raster; below: elevation-colored laser point cloud with intensity shading over the bare earth raster)

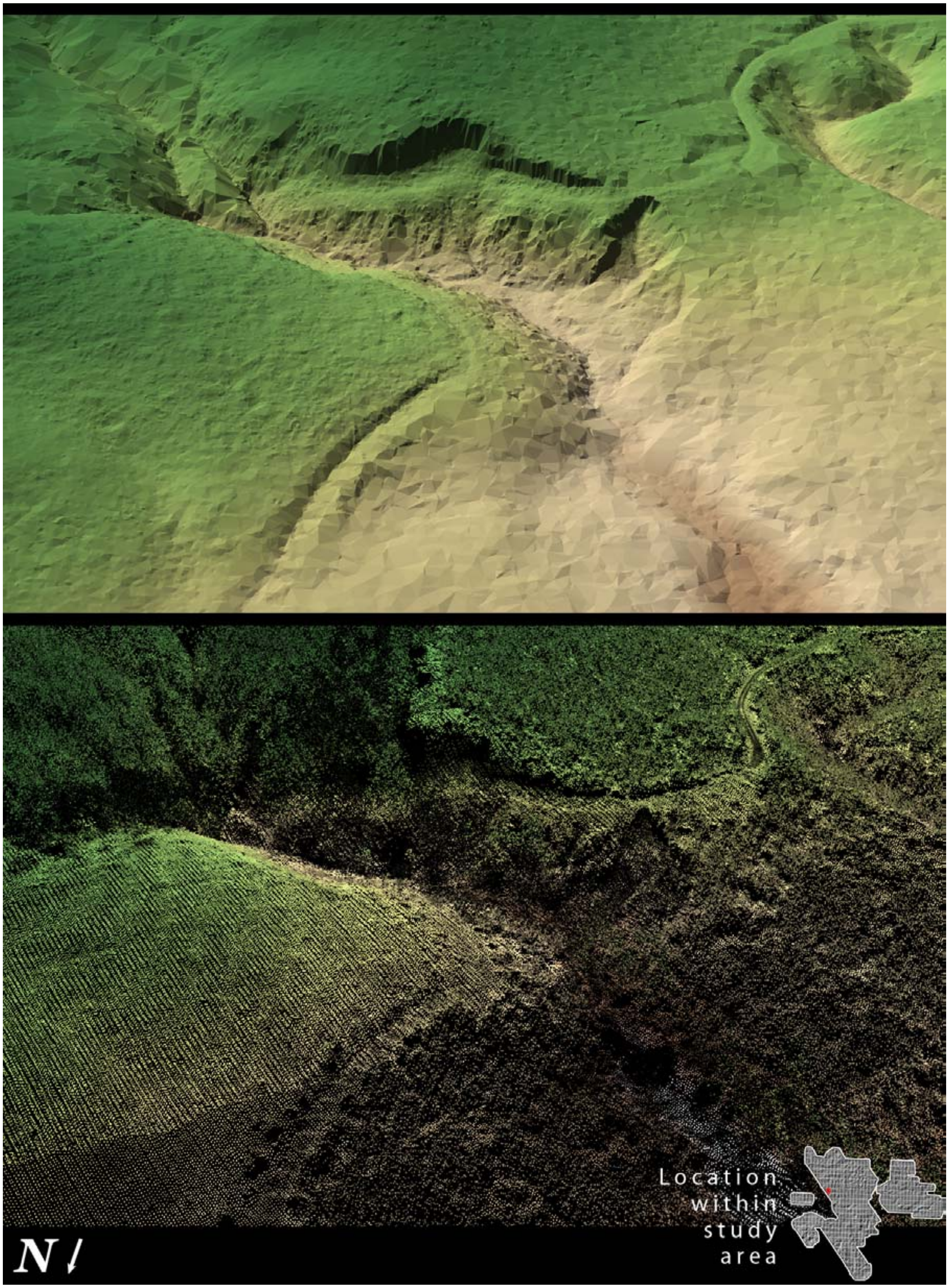

Figure 28. Paired 3-d oblique images of 46123-f3-sw-dc (above: elevation-colored, 0.5-foot resolution bare earth raster; below: elevation-colored laser point cloud with intensity shading over the bare earth raster)

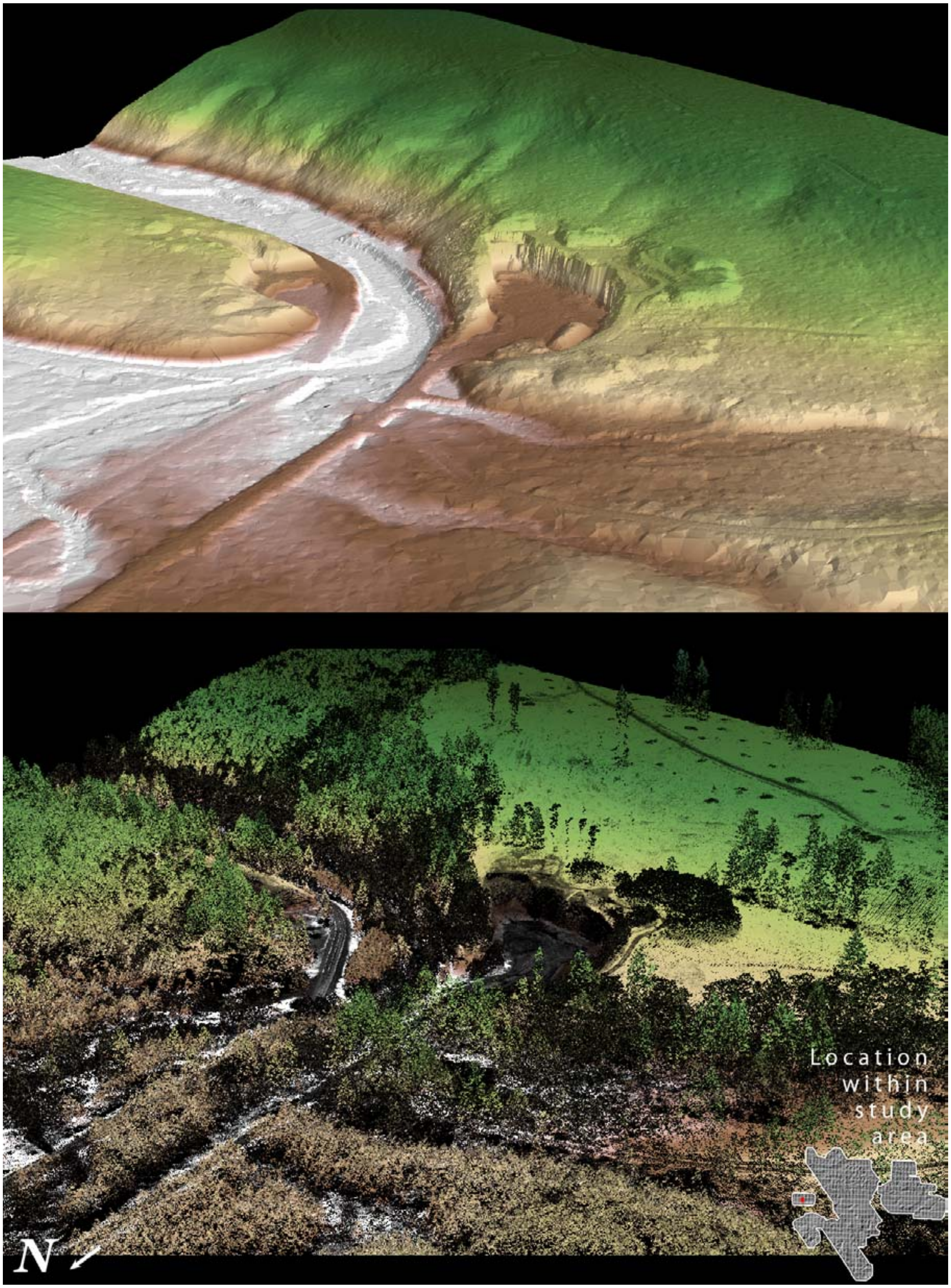

Figure 29. Paired 3-d oblique images of 46123-g2-se-bc (above: elevation-colored, 0.5-foot resolution bare earth raster; below: elevation-colored laser point cloud with intensity shading over the bare earth raster)

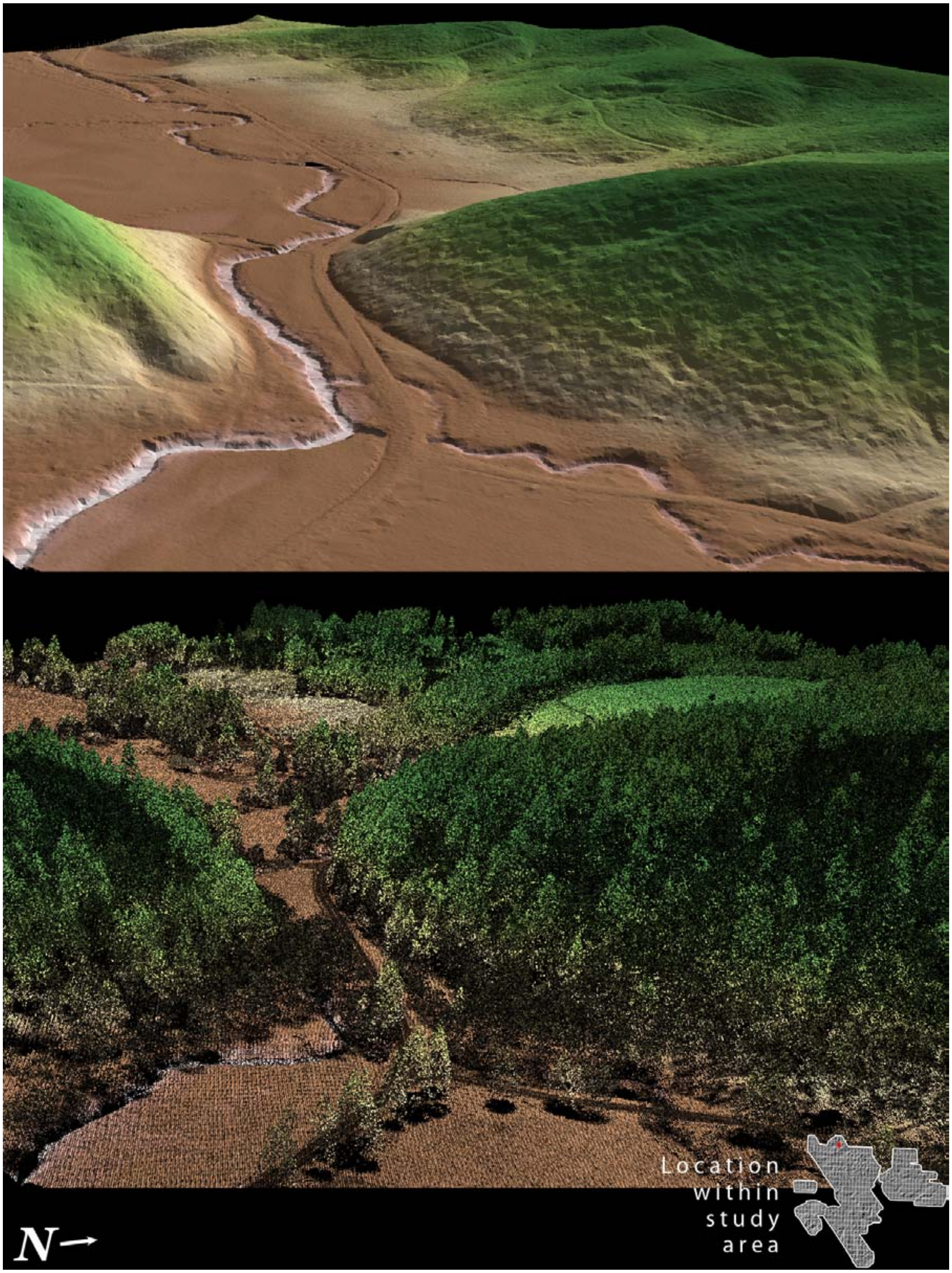

6. Glossary

1-sigma (σ) Absolute Deviation: Value for which the data are within one standard deviation (approximately 68th percentile) of a normally distributed data set.

2-sigma (σ) Absolute Deviation: Value for which the data are within two standard deviations (approximately 95th percentile) of a normally distributed data set.

Root Mean Square Error (RMSE): A statistic used to approximate the difference between real-world points and the LiDAR points. Calculated by squaring all the values, then taking the average of the squares and taking the square root of the average.

Pulse Repetition Frequency (PRF): The rate at which laser pulses are emitted from the sensor; typically measured as thousands of pulses per second (kHz).

Pulse Returns: For every laser emitted, the Optech ALTM 3100 LiDAR system can record *up to four* wave forms reflected back to the sensor. Portions of the wave form that return earliest are the highest element in multi-tiered surfaces such as vegetation. Portions of the wave form that return last are the lowest element in multi-tiered surfaces.

Accuracy: The statistical comparison between known (surveyed) points and laser points. Typically measured as the standard deviation (sigma, σ) and root mean square error (RMSE).

Intensity Values: The peak power ratio of the laser return to the emitted laser. It is a function of surface reflectivity.

Data Density: A common measure of LiDAR resolution, measured as points per square meter.

Spot Spacing: Also a measure of LiDAR resolution, measured as the average distance between laser points.

Nadir: A single point or locus of points on the surface of the earth directly below a sensor as it progresses along its flight line.

Scan Angle: The angle from nadir to the edge of the scan, measured in degrees. Laser point accuracy typically decreases as scan angles increase.

Overlap: The area shared between flight lines, typically measured in percents; 100% overlap is essential to ensure complete coverage and reduce laser shadows.

DTM / DEM: These often-interchanged terms refer to models made from laser points. The digital elevation model (DEM) refers to all surfaces, including bare ground and vegetation, while the digital terrain model (DTM) refers only to those points classified as ground.

Contours: Lines that represent known elevations with intervals typically recorded in feet. It is standard practice to develop minimum contour intervals with data that have two sigma accuracy.

Real-Time Kinematic (RTK) Survey: GPS surveying is conducted with a GPS base station deployed over a known monument with a radio connection to a GPS rover. Both the base station and rover receive differential GPS data and the baseline correction is solved between the two. This type of ground survey is accurate to 1.5 cm or less.

7. Citations

Andersen, H., R. McGaughey, W. Carson, S. Reutebuch, B. Mercer and J. Allan. 2003. A comparison of forest canopy models derived from LiDAR and INSAR data in a Pacific Northwest conifer forest. In: Proceedings of the ISPRS working group III/3 workshop '3-D reconstruction from airborne laserscanner and InSAR data'. Dresden, Germany.

Haugerud, R.A., and D. J. Harding. 2001. Some algorithms for virtual deforestation (VDF) of LiDAR topographic survey data. International Archives of Photogrammetry and Remote Sensing. XXXIV-3/W4, p. 211–217. duff.geology.washington.edu/data/raster/LiDAR/vdf4.pdf (March 2003).

McGaughey, R. And W. Carson. 2003. Fusing LiDAR data, photographs, and other data using 2D and 3D visualization techniques. In: Proceedings of Terrain Data: Applications and Visualization – Making the Connection. Charleston, South Carolina: Bethesda, MD: American Society for Photogrammery and Remote Sensing. 16-24.

Soininen, A. 2004. TerraScan User's Guide. Terrasolid.